Mathematics

https://www.aimspress.com/journal/Math

AIMS Mathematics, 10(12): 29380–29405.
DOI: 10.3934/math.20251290
Received: 01 June 2025
Revised: 7 November 2025
Accepted: 18 November 2025
Published: 12 December 2025

Research article

Numerical treatment for multi-pantograph integro-differential equation via tau spectral method

Samer S. Ezz-Eldien[1,*], Ali H. Tedjani[2], Faizah A. H. Alomari[3] and Amra Al Kenany[4]

[1] Department of Mathematics, Faculty of Science, New Valley University, El-Kharga, 72511, Egypt
[2] Department of Mathematics and Statistics, College of Science, Imam Mohammad Ibn Saud Islamic University (IMSIU), Riyadh, Saudi Arabia
[3] Department of Mathematics, Faculty of Science, Al-Baha University, Al-Baha 65779, Saudi Arabia
[4] Mathematics Department, Al-Qunfudah University College, Umm Al-Qura University, Mecca, KSA

* **Correspondence:** Email: s_sezeldien@yahoo.com.

Abstract: Pantograph integro-differential equations have many crucial applications in science and engineering. The presence of differential behavior, scaling, and memory effects makes pantograph integro-differential equations capable of describing complex systems in control theory and mathematical biology. In this paper, we provide a numerical approach to the multi-pantograph integro-differential equation. The Jacobi tau spectral approach is utilized with the help of differential, integral, and pantograph operational matrices to solve one- and two-dimensional linear multi-pantograph integro-differential equations. The high accuracy, convergence, and simplicity motivate one to apply the tau spectral approach to the problem studied. Numerical results for two test problems are performed to test the validity and superiority of the suggested numerical scheme over other numerical schemes.

Keywords: operational matrix; Jacobi polynomial; pantograph equation
Mathematics Subject Classification: 65L05, 65R20, 65N35, 65L03

1. Introduction

It is known that the pantograph integro-differential equation serves as a critical tool for analyzing and interpreting many real-world processes [1–3]. The pantograph integro-differential equation is a fusion of the integro-differential equation, and the pantograph equation enables it to be a powerful tool for dealing with processes including feedback, scaling, and memory effects [4–6]. These features ensure the relevance of the pantograph integro-differential equation in modeling the dynamics of populations according to the age distribution and processes of biological evolution, where the current behavior of the system depends on its historical behaviors at varying scales. In addition, the pantograph integro-differential equation can help optimize and design systems that involve scaling and delayed feedback like communication and robots systems [7–10].

Adding a pantograph term to the integro-differential equation doubles the difficulty of getting its exact solution, so the search for an efficient numerical solution for pantograph integro-differential equations is the main goal of a large number of researchers. In [11], the Sinc collocation approach was applied for the pantograph delay-integro-differential equation. The Galerkin spectral approach was implemented by the authors of [12, 13] to deal with a class of partial differential and integral equations with arbitrary orders. For the solution of linear pantograph delay-integro-differential equation, the authors of [14] implemented Bernstein tau spectral (BTS) and Lagrange interpolation collocation (LIC) approaches. The authors of [15] carried out the multivariate Jacobi approximation collocation for multi-dimensional weakly singular nonlinear integral equations with nonsmooth solutions. The bilinear neural network method can be used for various types of partial integral and differential equations [16–18], and neural network-based symbolic techniques are also applied to pantograph-type delay partial differential equations [19, 20]. Ji et al. [21] derived derivative and pantograph operational matrices that are used as the basis of the Chebyshev spectral collocation method (CSCM) to solve pantograph integro-differential equations. The pantograph nonlinear fractional integro-differential equation was solved by Jafari et al. [22] using the operational technique based on Legendre polynomials. Wang et al. [23] applied an operational procedure for a high-order nonlinear two-dimensional integro-differential equation based on Jacobi polynomials. Darania and Sotoudehmaram [24] adopted the multistep collocation technique as a numerical solution for nonlinear delay integral equations. In recent years, the interest in finding numerical solutions of different types of pantograph integro-differential equations has grown, see [25–27].

Our fundamental goal here is to introduce a numerical solution for the multi-pantograph integro-differential equation. To deal with the pantograph term, we present the shifted Jacobi polynomial-based pantograph operational matrix. Trying to make the computations simpler and faster, the shifted Jacobi Gauss quadrature method is employed for approximating the source term of the considered problem. Moreover, the operational matrix of integration is used to approximate the integral terms of the problem considered. On the other hand, we apply the same numerical technique for the two-dimensional multi-pantograph integro-differential equation and introduce the necessary operational matrices.

The rest of this manuscript is arranged as follows: In Section 2, we obtain some of the properties needed for shifted Jacobi polynomials. In Section 3, we introduce the shifted Jacobi polynomial-based pantograph, and the integration and differentiation operational matrices that are combined with the Gauss quadrature and spectral tau approaches to solve the multi-pantograph integro-differential equation. In Section 4, an extension of the numerical scheme discussed in the previous section for the Volterra-type integro-differential equation with variable kernels is presented. In Section 5, the numerical approach introduced in Section 3 is employed for the system of multi-pantograph integro-differential equations. In Section 6, we extend the application of the presented numerical technique to the two-dimensional multi-pantograph integro-differential equation. In Section 7, we carry out a convergence analysis of the numerical scheme proposed in Section 3. In Section 8, comparisons with the numerical results achieved by spectral methods in the literature are made. In Section 9, some concluding remarks are highlighted.

2. Shifted Jacobi polynomials

The shifted Jacobi polynomials defined in $[0, \alpha]$, denoted by $S_{\alpha,l}^{(a,b)}(x)$, $l = 0, 1, \cdots$, can be expressed as

$$S_{\alpha,l}^{(a,b)}(x) = \sum_{i=0}^{l} \mathcal{E}_{l,i}\, x^i = \sum_{i=0}^{l} \frac{(-1)^{l-i}\Gamma(l+b+1)\Gamma(l+i+a+b+1)}{\Gamma(i+b+1)\Gamma(l+a+b+1)l!(l-i)!\alpha^l} x^i,$$

and satisfy

$$\frac{d^q}{dx^q} S_{\alpha,l}^{(a,b)}(0) = (-1)^{l-q} \frac{\Gamma(l+b+1)(l+a+b+1)_q}{\Gamma(l-q+1)\Gamma(q+b+1)\alpha^q}.$$

The shifted Jacobi polynomials satisfy the orthogonality relation

$$\int_0^\alpha S_{\alpha,l}^{(a,b)}(x) S_{\alpha,m}^{(a,b)}(x) w_\alpha^{(a,b)}(x) dx = h_{\alpha,l}^{(a,b)} \delta_{lm},$$

where $w_\alpha^{(a,b)}(x) = x^b(\alpha - x)^a$, $h_{\alpha,l}^{(a,b)} = \dfrac{\alpha^{a+b+1}\Gamma(l+a+1)\Gamma(l+b+1)}{(2l+a+b+1)l!\Gamma(l+a+b+1)}$ and δ_{lm} is the well-known Kronecker delta function.
Any function $f \in L^2(\Lambda_x)$ can be expanded on the basis of the shifted Jacobi polynomials as follows:

$$f(x) = \sum_{l=0}^{\infty} f_l S_{\alpha,l}^{(a,b)}(x); \qquad f_l = \frac{1}{h_{\alpha,l}^{(a,b)}} \int_0^\alpha f(x) S_{\alpha,l}^{(a,b)}(x) w_\alpha^{(a,b)}(x) dx. \tag{2.1}$$

If we denote $P_{\mathcal{L}}^\alpha$ by the orthogonal projection:

$$P_{\mathcal{L}}^\alpha : L^2(\Lambda_x) \to \mathcal{S}_{\mathcal{L}}^\alpha; \qquad \mathcal{S}_{\mathcal{L}}^\alpha = \text{Span}\{S_{\alpha,l}^{(a,b)}(x) : \quad 0 \le l \le \mathcal{L}\},$$

we then have

$$P_{\mathcal{L}}^\alpha f = f_{\mathcal{L}}(x) = \sum_{l=0}^{\mathcal{L}} f_l S_{\alpha,l}^{(a,b)}(x) = \mathcal{F}_{\mathcal{L}}^T \mathfrak{S}_{\alpha,\mathcal{L}}(x), \tag{2.2}$$

where

$$\mathcal{F}_{\mathcal{L}} = \begin{bmatrix} f_0 \\ f_1 \\ \vdots \\ f_{\mathcal{L}} \end{bmatrix}_{((\mathcal{L}+1)\times 1)} \qquad \mathfrak{S}_{\alpha,\mathcal{L}}(x) = \begin{bmatrix} S_{\alpha,0}^{(a,b)}(x) \\ S_{\alpha,1}^{(a,b)}(x) \\ \vdots \\ S_{\alpha,\mathcal{L}}^{(a,b)}(x) \end{bmatrix}_{((\mathcal{L}+1)\times 1)}. \tag{2.3}$$

Similarly, for $f \in L^2(\Lambda_x \times \Lambda_y)$ and $\Lambda_x = [0, \alpha]$, and $\Lambda_y = [0, \beta]$, we have

$$f_{\mathcal{L},\mathcal{M}}(x, y) = \sum_{l=0}^{\mathcal{L}} \sum_{m=0}^{\mathcal{M}} f_{i,j} S_{\alpha,l}^{(a,b)}(x) S_{\beta,m}^{(a,b)}(y) = \mathcal{F}_{\mathcal{L},\mathcal{M}}^T \mathfrak{S}_{\mathcal{L},\mathcal{M}}^{\alpha,\beta}(x, y), \tag{2.4}$$

where $\mathcal{F}_{\mathcal{L},\mathcal{M}}$ and $\mathfrak{S}^{\alpha,\beta}_{\mathcal{L},\mathcal{M}}(x,y)$ are defined by

$$\mathcal{F}_{\mathcal{L},\mathcal{M}} = \begin{bmatrix} f_{0,0} \\ f_{0,1} \\ \vdots \\ f_{0,\mathcal{M}} \\ f_{1,0} \\ \vdots \\ f_{\mathcal{L},\mathcal{M}} \end{bmatrix}_{((\mathcal{L}+1)(\mathcal{M}+1)\times 1)} \qquad \mathfrak{S}^{\alpha,\beta}_{\mathcal{L},\mathcal{M}}(x,y) = \begin{bmatrix} S^{(a,b)}_{\alpha,0}(x)S^{(a,b)}_{\beta,0}(y) \\ S^{(a,b)}_{\alpha,0}(x)S^{(a,b)}_{\beta,1}(y) \\ \vdots \\ S^{(a,b)}_{\alpha,0}(x)S^{(a,b)}_{\beta,\mathcal{M}}(y) \\ S^{(a,b)}_{\alpha,1}(x)S^{(a,b)}_{\beta,0}(y) \\ \vdots \\ S^{(a,b)}_{\alpha,\mathcal{L}}(x)S^{(a,b)}_{\beta,\mathcal{M}}(y) \end{bmatrix}_{((\mathcal{L}+1)(\mathcal{M}+1)\times 1)}, \tag{2.5}$$

and

$$f_{l,m} = \frac{1}{h^{(a,b)}_{\alpha,l} h^{(a,b)}_{\beta,m}} \int_0^\alpha \int_0^\beta f(x,y) S^{(a,b)}_{\alpha,l}(x) S^{(a,b)}_{\beta,m}(y) w^{(a,b)}_{\alpha}(x) w^{(a,b)}_{\beta}(y) dxdy. \tag{2.6}$$

3. Multi-pantograph integro-differential equation

In this section, we study the application of Jacobi's spectral method for the multi-pantograph integro-differential equation in the following form:

$$\frac{d}{dx} f(x) + \sum_{i=0}^{s} \gamma_i f(c_i x) = g(x) + \sum_{i=0}^{s} \int_0^{c_i x} \mu_i f(t) dt + \int_0^x \nu f(t) dt, \qquad 0 \le x \le \alpha, \tag{3.1}$$

where $f(0) = \theta$ and $\nu,\ \theta,\ \gamma_i,\ \mu_i,\ c_i;\ (0 < c_i < 1,\ 0 \le i \le s)$ are known real numbers.
The considered approach is to find $f_{\mathcal{L}} \in \mathcal{S}^{\alpha}_{\mathcal{L}}$, such that

$$\frac{d}{dx} f_{\mathcal{L}}(x) + \sum_{i=0}^{s} \gamma_i f_{\mathcal{L}}(c_i x) = g_{\mathcal{L}}(x) + \sum_{i=0}^{s} \int_0^{c_i x} \mu_i f_{\mathcal{L}}(t) dt + \int_0^x \nu f_{\mathcal{L}}(t) dt. \tag{3.2}$$

Define

$$\begin{aligned} f_{\mathcal{L}}(x) &= \mathcal{F}^T_{\mathcal{L}} \mathfrak{S}_{\alpha,\mathcal{L}}(x), \\ g_{\mathcal{L}}(x) &= \mathcal{G}^T_{\mathcal{L}} \mathfrak{S}_{\alpha,\mathcal{L}}(x), \end{aligned} \tag{3.3}$$

where $\mathcal{F}_{\mathcal{L}}$ and $\mathfrak{S}_{\alpha,\mathcal{L}}(x)$ are given in (2.3), and

$$\mathcal{G}_{\mathcal{L}} = \begin{bmatrix} g_0 \\ g_1 \\ \vdots \\ g_{\mathcal{L}} \end{bmatrix}_{((\mathcal{L}+1)\times 1)} ; \qquad g_j = \frac{1}{h^{(a,b)}_{\alpha,j}} \sum_{k=0}^{\mathcal{L}} W^{(a,b)}_{\mathcal{L},k,\alpha} g\left(x^{(a,b)}_{\mathcal{L},k,\alpha}\right) S^{(a,b)}_{\alpha,j}\left(x^{(a,b)}_{\mathcal{L},k,\alpha}\right),$$

where $x^{(a,b)}_{\mathcal{L},k,\alpha}$, $0 \le k \le \mathcal{L}$, are the shifted Jacobi Gauss quadrature nodes on $(0,\alpha)$, and $W^{(a,b)}_{\mathcal{L},k,\alpha}$ are the Christoffel numbers.

Lemma 1. *[28] The derivative of the vector $\Im_{\alpha,\mathcal{L}}(x)$ is given by*

$$\frac{d}{dx}\Im_{\alpha,\mathcal{L}}(x) = \boldsymbol{D}^{(1)}_{\mathcal{L}}\Im_{\alpha,\mathcal{L}}(x), \tag{3.4}$$

with

$$\boldsymbol{D}^{(1)}_{\mathcal{L}} = (d_{l,m})_{0\le l,m\le\mathcal{L}}; \qquad d_{l,m} = \begin{cases} C_1(l,m), & m < l, \\ 0, & \textit{otherwise}, \end{cases}$$

and

$$C_1(l,m) = \frac{\alpha^{a+b}(l+a+b+1)(l+a+b+2)_m(m+a+2)_{l-m-1}\Gamma(m+a+b+1)}{(l-m-1)!\Gamma(2m+a+b+1)} \times {}_3F_2\left(\begin{matrix} -l+1+m, & l+m+a+b+2, & m+a+1 \\ m+a+2, & 2m+a+b+2 & \end{matrix} ;1\right).$$

Lemma 2. *[29] The integration of the vector $\Im_{\alpha,\mathcal{L}}(x)$ is given by:*

$$\int_0^x \Im_{\alpha,\mathcal{L}}(x)dx = \boldsymbol{I}^{(1)}_{\mathcal{L}}\Im_{\alpha,\mathcal{L}}(x), \tag{3.5}$$

where

$$\boldsymbol{I}^{(1)}_{\mathcal{L}} = (I_{l,m})_{0\le l,m\le\mathcal{L}},$$

and

$$I_{l,m} = \sum_{k=0}^{l}\frac{(-1)^{l-k}\Gamma(l+b+1)\Gamma(l+k+a+b+1)\alpha}{\Gamma(k+b+1)\Gamma(m+a+b+1)(l-k)!\Gamma(k+2)} \times \sum_{l=0}^{m}\frac{(-1)^{m-l}\Gamma(m+l+a+b+1)\Gamma(a+1)\Gamma(l+k+b+2)(2m+a+b+1)m!}{\Gamma(m+a+1)\Gamma(l+b+1)(m-l)!l!\Gamma(l+k+a+b+3)}.$$

Theorem 1. *For $0 \le c \le 1$, the pantograph operational matrix $\boldsymbol{P}_{\mathcal{L},c}$ is given by*

$$\Im_{\alpha,\mathcal{L}}(cx) = \boldsymbol{P}_{\mathcal{L},c}\Im_{\alpha,\mathcal{L}}(x), \tag{3.6}$$

where $\boldsymbol{P}_{\mathcal{L},c} = (\boldsymbol{p}^c_{l,j})_{0\le l,j\le\mathcal{L}}$, and $\boldsymbol{p}^c_{l,j} = \sum_{k=0}^{l}\mathcal{E}_{l,k}c^k q_{k,j}$.

Proof. We start by expressing $\mathcal{S}^{a,b}_{\alpha,l}(cx)$ as follows:

$$S^{(a,b)}_{\alpha,l}(cx) = \sum_{i=0}^{l}\mathcal{E}_{l,i}\,c^i x^i. \tag{3.7}$$

We expand x^i in terms of $\mathcal{S}^{(a,b)}_{\alpha,j}(x)$, $j = 0,1,\cdots,\mathcal{L}$, as follows:

$$x^i = \sum_{j=0}^{\mathcal{L}} q_{i,j}\mathcal{S}^{(a,b)}_{\alpha,j}(x); \qquad q_{i,j} = \frac{1}{h^{(a,b)}_{\alpha,j}}\int_0^\alpha x^i\mathcal{S}^{(a,b)}_{\alpha,j}(x)w^{(a,b)}_\alpha(x)dx. \tag{3.8}$$

A combination of (3.7) and (3.8) then yields

$$\begin{aligned} S_{\alpha,l}^{(a,b)}(cx) &= \sum_{i=0}^{l} \mathcal{E}_{l,i} c^i \left(\sum_{j=0}^{\mathcal{L}} q_{i,j} \mathcal{S}_{\alpha,j}^{(a,b)}(x) \right) = \sum_{j=0}^{\mathcal{L}} \mathcal{S}_{\alpha,j}^{(a,b)} \left(\sum_{i=0}^{l} \mathcal{E}_{l,i} c^i q_{i,j} \right) \\ &= \left[\sum_{i=0}^{l} \mathcal{E}_{l,i} c^i q_{i,0},\ \sum_{i=0}^{l} \mathcal{E}_{l,i} c^i q_{i,1},\ \cdots,\ \sum_{i=0}^{l} \mathcal{E}_{l,i} c^i q_{i,\mathcal{L}} \right]^T \mathfrak{S}_{\alpha,\mathcal{L}}(x), \end{aligned} \tag{3.9}$$

which completes the proof. □

Through Lemmas 1, 2 and Theorem 1, we get

$$\begin{aligned} \frac{d f_{\mathcal{L}}(x)}{dx} &= \mathcal{F}_{\mathcal{L}}^T \mathbf{D}_{\mathcal{L}}^{(1)} \mathfrak{S}_{\alpha,\mathcal{L}}(x), \\ \int_0^x f_{\mathcal{L}}(t)dt &= \mathcal{F}_{\mathcal{L}}^T \mathbf{I}_{\mathcal{L}}^{(1)} \mathfrak{S}_{\alpha,\mathcal{L}}(x), \\ f_{\mathcal{L}}(cx) &= \mathcal{F}_{\mathcal{L}}^T \mathbf{P}_{\mathcal{L},c} \mathfrak{S}_{\alpha,\mathcal{L}}(x), \\ \int_0^{cx} f_{\mathcal{L}}(t)dt &= \mathcal{F}_{\mathcal{L}}^T \mathbf{I}_{\mathcal{L}}^{(1)} \mathbf{P}_{\mathcal{L},c} \mathfrak{S}_{\alpha,\mathcal{L}}(x). \end{aligned} \tag{3.10}$$

Using (3.10), the residual $\mathcal{R}_{\mathcal{L}}(x)$ for (3.2) is given by

$$\begin{aligned} \mathcal{R}_{\mathcal{L}}(x) = \mathcal{F}_{\mathcal{L}}^T \mathbf{D}_{\mathcal{L}}^{(1)} \mathfrak{S}_{\alpha,\mathcal{L}}(x) &+ \sum_{i=0}^{s} \gamma_i \mathcal{F}_{\mathcal{L}}^T \mathbf{P}_{\mathcal{L},c_i} \mathfrak{S}_{\alpha,\mathcal{L}}(x) - \mathcal{G}_{\mathcal{L}}^T \mathfrak{S}_{\alpha,\mathcal{L}}(x) \\ &- \sum_{i=0}^{s} \mu_i \mathcal{F}_{\mathcal{L}}^T \mathbf{I}_{\mathcal{L}}^{(1)} \mathbf{P}_{\mathcal{L},c_i} \mathfrak{S}_{\alpha,\mathcal{L}}(x) - \nu \mathcal{F}_{\mathcal{L}}^T \mathbf{I}_{\mathcal{L}}^{(1)} \mathfrak{S}_{\alpha,\mathcal{L}}(x). \end{aligned} \tag{3.11}$$

We now generate a system of $\mathcal{L}+1$ algebraic equations in the unknowns as follows:

$$\begin{cases} \int_0^{\alpha} \mathcal{R}_{\mathcal{L}}(t) w_{\alpha}^{(a,b)} \mathcal{S}_{\alpha,0}^{(a,b)}(t) dt = 0, \\ \int_0^{\alpha} \mathcal{R}_{\mathcal{L}}(t) w_{\alpha}^{(a,b)} \mathcal{S}_{\alpha,1}^{(a,b)}(t) dt = 0, \\ \qquad \vdots \\ \int_0^{\alpha} \mathcal{R}_{\mathcal{L}}(t) w_{\alpha}^{(a,b)} \mathcal{S}_{\alpha,\mathcal{L}-1}^{(a,b)}(t) dt = 0, \\ \mathcal{F}_{\mathcal{L}}^T \mathfrak{S}_{\alpha,\mathcal{L}}(0) = \theta. \end{cases} \tag{3.12}$$

Define the vector ${}_{\alpha}\mathbf{O}_{\mathcal{L}}^{i},\ i = 0, 1, \cdots, \mathcal{L}-1$, as follows:

$${}_{\alpha}\mathbf{O}_{\mathcal{L}}^{i} = \left[\overbrace{0, 0, \cdots, 0}^{i}, \frac{1}{h_{\alpha,i}^{(a,b)}}, \overbrace{0, 0, \cdots, 0}^{\mathcal{L}-i} \right]^T. \tag{3.13}$$

The system (3.12) simplifies to

$$\mathcal{F}_{\mathcal{L}}^T \mathbf{D}_{\mathcal{L}}^{(1)} {}_{\alpha}\mathbf{O}_{\mathcal{L}}^{i} + \sum_{i=0}^{s} \gamma_i \mathcal{F}_{\mathcal{L}}^T \mathbf{P}_{\mathcal{L},c_i} {}_{\alpha}\mathbf{O}_{\mathcal{L}}^{i} - \sum_{i=0}^{s} \mu_i \mathcal{F}_{\mathcal{L}}^T \mathbf{I}_{\mathcal{L}}^{(1)} \mathbf{P}_{\mathcal{L},c_i} {}_{\alpha}\mathbf{O}_{\mathcal{L}}^{i} - \nu \mathcal{F}_{\mathcal{L}}^T \mathbf{I}_{\mathcal{L}}^{(1)} {}_{\alpha}\mathbf{O}_{\mathcal{L}}^{i} - \mathcal{G}_{\mathcal{L}}^T {}_{\alpha}\mathbf{O}_{\mathcal{L}}^{i} = 0, \tag{3.14}$$

with $i = 0, 1, \cdots, \mathcal{L} - 1$.
If we denote $C = (\mathfrak{S}_{\alpha,\mathcal{L}}(0))^T$ and $M_i,\ i = 0, 1, \cdots, \mathcal{L} - 1$ as

$$M_i = \left({}_{\alpha}\mathbf{O}^i_{\mathcal{L}}\right)^T \left(\mathbf{D}^{(1)}_{\mathcal{L}}\right)^T + \sum_{i=0}^{s} \gamma_i \left({}_{\alpha}\mathbf{O}^i_{\mathcal{L}}\right)^T - \sum_{i=0}^{s} \mu_i \left({}_{\alpha}\mathbf{O}^i_{\mathcal{L}}\right)^T \mathbf{P}^T_{\mathcal{L},c_i} \left(\mathbf{I}^{(1)}_{\mathcal{L}}\right)^T - \nu \left({}_{\alpha}\mathbf{O}^i_{\mathcal{L}}\right)^T \left(\mathbf{I}^{(1)}_{\mathcal{L}}\right)^T,$$

then the solution of (3.1) is reduced to the system

$$\mathbf{E}\mathcal{F}_{\mathcal{L}} = \mathbf{R},$$

where

$$\begin{aligned}
\mathbf{E} &= \left[M_0,\ M_1,\ \cdots,\ M_{\mathcal{L}-1},\ C\right], \\
\mathbf{R} &= \left[\frac{g_0}{h^{(a,b)}_{\alpha,0}},\ \frac{g_1}{h^{(a,b)}_{\alpha,1}},\ \frac{g_2}{h^{(a,b)}_{\alpha,2}},\ \cdots,\ \frac{g_{\mathcal{L}-1}}{h^{(a,b)}_{\alpha,\mathcal{L}-1}},\ \theta\right]^T.
\end{aligned}$$

4. Multi-pantograph Volterra-type integro-differential equations with variable kernel functions

Here, we apply the Jacobi spectral method for a more complex extension of the multi-pantograph integro-differential Eq (3.1) by incorporating variable kernels as follows:

$$\frac{d}{dx}f(x) + \sum_{i=0}^{s} \gamma_i f(c_i x) = g(x) + \sum_{i=0}^{s} \int_0^{c_i x} K^{(1,i)}(x,t) f(t)dt + \int_0^{x} K^{(2)}(x,t) f(t)dt, \qquad 0 \le x \le \alpha, \quad (4.1)$$

where $f(0) = \theta$ and $\nu,\ \theta,\ \gamma_i,\ \mu_i,\ c_i;\ (0 < c_i < 1,\ 0 < i < s)$ are known real numbers.
First, we approximate $f(x)$ and $g(x)$ as (3.3), and the kernels $K_{1,i}(x,t),\ 0 \le i \le s$, and $K_2(x,t)$ as follows:

$$\begin{aligned}
K^{(1,i)}_{\mathcal{L}}(x,t) &= \mathfrak{S}^T_{\alpha,\mathcal{L}}(x)\mathcal{K}^{(1,i)}_{\mathcal{L}}\mathfrak{S}_{\alpha,\mathcal{L}}(t), \\
K^{(2)}_{\mathcal{L}}(x,t) &= \mathfrak{S}^T_{\alpha,\mathcal{L}}(x)\mathcal{K}^{(2)}_{\mathcal{L}}\mathfrak{S}_{\alpha,\mathcal{L}}(t),
\end{aligned} \qquad (4.2)$$

with

$$\mathcal{K}^{(1,i)}_{\mathcal{L}} = \begin{pmatrix} k^{(1,i)}_{0,0} & k^{(1,i)}_{0,1} & \cdots & k^{(1,i)}_{0,\mathcal{L}} \\ k^{(1,i)}_{1,0} & k^{(1,i)}_{1,1} & \cdots & k^{(1,i)}_{1,\mathcal{L}} \\ \vdots & \vdots & \ddots & \vdots \\ k^{(1,i)}_{\mathcal{L},0} & k^{(1,i)}_{\mathcal{L},1} & \cdots & k^{(1,i)}_{\mathcal{L},\mathcal{L}} \end{pmatrix}, \qquad \mathcal{K}^{(2)}_{\mathcal{L}} = \begin{pmatrix} k^{(2)}_{0,0} & k^{(2)}_{0,1} & \cdots & k^{(2)}_{0,\mathcal{L}} \\ k^{(2)}_{1,0} & k^{(2)}_{1,1} & \cdots & k^{(2)}_{1,\mathcal{L}} \\ \vdots & \vdots & \ddots & \vdots \\ k^{(2)}_{\mathcal{L},0} & k^{(2)}_{\mathcal{L},1} & \cdots & k^{(2)}_{\mathcal{L},\mathcal{L}} \end{pmatrix},$$

and

$$\begin{aligned}
k^{(1,i)}_{j,k} &= \frac{1}{h^{(a,b)}_{\alpha,j} h^{(a,b)}_{\alpha,k}} \int_0^{\alpha}\int_0^{\alpha} S^{(a,b)}_{\alpha,j}(x) S^{(a,b)}_{\alpha,k}(t) w^{(a,b)}_{\alpha}(x) w^{(a,b)}_{\alpha}(t) K^{(1,i)}(x,t)dtdx \\
&= \frac{1}{h^{(a,b)}_{\alpha,j} h^{(a,b)}_{\alpha,k}} \sum_{r=0}^{\mathcal{L}}\sum_{s=0}^{\mathcal{L}} W^{(a,b)}_{\mathcal{L},r,\alpha} W^{(a,b)}_{\mathcal{L},s,\alpha} K^{(1,i)}\left(x^{(a,b)}_{\mathcal{L},r,\alpha}, x^{(a,b)}_{\mathcal{L},s,\alpha}\right) S^{(a,b)}_{\alpha,j}\left(x^{(a,b)}_{\mathcal{L},r,\alpha}\right) S^{(a,b)}_{\alpha,k}\left(x^{(a,b)}_{\mathcal{L},s,\alpha}\right), \\
k^{(2)}_{j,k} &= \frac{1}{h^{(a,b)}_{\alpha,j} h^{(a,b)}_{\alpha,k}} \int_0^{\alpha}\int_0^{\alpha} S^{(a,b)}_{\alpha,j}(x) S^{(a,b)}_{\alpha,k}(t) w^{(a,b)}_{\alpha}(x) w^{(a,b)}_{\alpha}(t) K^{(2)}(x,t)dtdx \\
&= \frac{1}{h^{(a,b)}_{\alpha,j} h^{(a,b)}_{\alpha,k}} \sum_{r=0}^{\mathcal{L}}\sum_{s=0}^{\mathcal{L}} W^{(a,b)}_{\mathcal{L},r,\alpha} W^{(a,b)}_{\mathcal{L},s,\alpha} K^{(2)}\left(x^{(a,b)}_{\mathcal{L},r,\alpha}, x^{(a,b)}_{\mathcal{L},s,\alpha}\right) S^{(a,b)}_{\alpha,j}\left(x^{(a,b)}_{\mathcal{L},r,\alpha}\right) S^{(a,b)}_{\alpha,k}\left(x^{(a,b)}_{\mathcal{L},s,\alpha}\right).
\end{aligned} \qquad (4.3)$$

Then, we have to find $f_{\mathcal{L}} \in \mathcal{S}_{\mathcal{L}}^{\alpha}$, such that

$$\frac{d}{dx} f_{\mathcal{L}}(x) + \sum_{i=0}^{s} \gamma_i f_{\mathcal{L}}(c_i x) = g_{\mathcal{L}}(x) + \sum_{i=0}^{s} \int_0^{c_i x} K_{\mathcal{L}}^{(1,i)}(x,t) f_{\mathcal{L}}(t) dt + \int_0^x K_{\mathcal{L}}^{(2)}(x,t) f_{\mathcal{L}}(t) dt. \tag{4.4}$$

In this regard, we have

$$\begin{aligned} \int_0^{c_i x} K_{\mathcal{L}}^{(1,i)}(x,t) f_{\mathcal{L}}(t) dt &= \int_0^{c_i x} \left(\mathfrak{S}_{\alpha,\mathcal{L}}^T(x) \mathcal{K}_{\mathcal{L}}^{(1,i)} \mathfrak{S}_{\alpha,\mathcal{L}}(t) \right) \left(\mathcal{F}_{\mathcal{L}}^T \mathfrak{S}_{\alpha,\mathcal{L}}(x) \right) dt \\ &= \int_0^{c_i x} \mathfrak{S}_{\alpha,\mathcal{L}}^T(x) \mathcal{K}_{\mathcal{L}}^{(1,i)} \mathfrak{S}_{\alpha,\mathcal{L}}(t) \mathfrak{S}_{\alpha.\mathcal{L}}^T(x) \mathcal{F}_{\mathcal{L}} dt \\ &\simeq \int_0^{c_i x} \mathfrak{S}_{\alpha,\mathcal{L}}^T(x) \mathcal{K}_{\mathcal{L}}^{(1,i)} \mathcal{H}^T \mathfrak{S}_{\alpha,\mathcal{L}}(t) dt, \end{aligned} \tag{4.5}$$

with

$$\begin{aligned} \mathcal{H} = \left(H_{i,j} \right)_{0 \le i,j \le \mathcal{L}}; \quad H_{i,j} &= \frac{1}{h_{\alpha,i}^{(a,b)}} \sum_{k=0}^{\mathcal{L}} \left(f_i \int_0^{\alpha} S_{\alpha,i}^{(a,b)}(t) S_{\alpha,j}^{(a,b)}(t) S_{\alpha,k}^{(a,b)}(t) w_{\alpha}^{(a,b)}(t) dt \right) \\ &= \frac{1}{h_{\alpha,i}^{(a,b)}} \sum_{k=0}^{\mathcal{L}} \left(f_i \sum_{r=0}^{\mathcal{L}} W_{\mathcal{L},r,\alpha}^{(a,b)} \mathcal{S}_{\alpha,i}^{(a,b)} \left(x_{\mathcal{L},r,\alpha}^{(a,b)} \right) \mathcal{S}_{\alpha,j}^{(a,b)} \left(x_{\mathcal{L},r,\alpha}^{(a,b)} \right) \mathcal{S}_{\alpha,k}^{(a,b)} \left(x_{\mathcal{L},r,\alpha}^{(a,b)} \right) \right). \end{aligned}$$

Similarly,

$$\int_0^x K_{\mathcal{L}}^{(2)}(x,t) f_{\mathcal{L}}(t) dt \simeq \int_0^x \mathfrak{S}_{\alpha,\mathcal{L}}^T(x) \mathcal{K}_{\mathcal{L}}^{(2)} \mathcal{H}^T \mathfrak{S}_{\alpha,\mathcal{L}}(t) dt. \tag{4.6}$$

Lemmas 1, 2 and Theorem 1 with Eqs (4.5) and (4.6) yield

$$\begin{aligned} \int_0^{c_i x} K_{\mathcal{L}}^{(1,i)}(x,t) f_{\mathcal{L}}(t) dt &\simeq \mathfrak{S}_{\alpha,\mathcal{L}}^T(x) \mathcal{K}_{\mathcal{L}}^{(1,i)} \mathcal{H}^T \mathbf{I}_{\mathcal{L}}^{(1)} \mathbf{P}_{\mathcal{L},c_i} \mathfrak{S}_{\alpha,\mathcal{L}}(x), \\ \int_0^x K_{\mathcal{L}}^{(2)}(x,t) f_{\mathcal{L}}(t) dt &\simeq \mathfrak{S}_{\alpha,\mathcal{L}}^T(x) \mathcal{K}_{\mathcal{L}}^{(2)} \mathcal{H}^T \mathbf{I}_{\mathcal{L}}^{(1)} \mathfrak{S}_{\alpha,\mathcal{L}}(x). \end{aligned} \tag{4.7}$$

Hence, the residual of (4.1) can be given by

$$\begin{aligned} \mathcal{R}_{\mathcal{L}}(x) = \mathcal{F}_{\mathcal{L}}^T \mathbf{D}_{\mathcal{L}}^{(1)} \mathfrak{S}_{\alpha,\mathcal{L}}(x) + \sum_{i=0}^{s} \gamma_i \mathcal{F}_{\mathcal{L}}^T \mathbf{P}_{\mathcal{L},c_i} \mathfrak{S}_{\alpha,\mathcal{L}}(x) - \mathcal{G}_{\mathcal{L}}^T \mathfrak{S}_{\alpha,\mathcal{L}}(x) \\ - \sum_{i=0}^{s} \mathfrak{S}_{\alpha,\mathcal{L}}^T(x) \mathcal{K}_{\mathcal{L}}^{(1,i)} \mathcal{H}^T \mathbf{I}_{\mathcal{L}}^{(1)} \mathbf{P}_{\mathcal{L},c_i} \mathfrak{S}_{\alpha,\mathcal{L}}(x) - \mathfrak{S}_{\alpha,\mathcal{L}}^T(x) \mathcal{K}_{\mathcal{L}}^{(2)} \mathcal{H}^T \mathbf{I}_{\mathcal{L}}^{(1)} \mathfrak{S}_{\alpha,\mathcal{L}}(x), \end{aligned} \tag{4.8}$$

Then a system of $\mathcal{L} + 1$ algebraic equations in the unknowns is generated as in (3.12).

5. The system of multi-pantograph integro-differential equations

This section is dedicated to applying the numerical approach studied in Section 3 to the system of multi-pantograph integro-differential equations

$$\frac{d f_l(x)}{dx} + \sum_{k=1}^{r} \sum_{i=0}^{s} \gamma_{l,k,i} f_k(c_{k,i} x) = g_l(x) + \sum_{k=1}^{r} \sum_{i=0}^{s} \int_0^{c_{k,i} x} \mu_{l,k,i} f_k(t) dt + \sum_{k=1}^{r} \int_0^x \nu_{l,k} f_k(t) dt, \tag{5.1}$$

where $f_l(0)=\theta_l$ and $0\le x\le\alpha,\ \gamma_{l,k,i},\ \mu_{l,k,i},\ \nu_{k,l},\ c_{k,i},\ \theta_l$ are known real numbers with $1\le k,l\le r,\ 0\le i\le s$, and $0<c_{k,i}<1$.
The problem (5.1) may be transformed to an equivalent problem of finding $\mathbf{F}(x)$, such that

$$\begin{cases} \dfrac{d\mathbf{F}(x)}{dx}+\sum_{i=0}^{s}\mathbf{A}_i\mathbf{F}(c_{i,l}x)=\mathbf{G}(x)+\sum_{i=0}^{s}\int_0^{c_{i,l}x}\mathbf{B}_i\mathbf{F}(w)dw+\int_0^x\mathbf{C}\,\mathbf{F}(w)dw,\\ \mathbf{F}(0)=\Theta,\end{cases}\tag{5.2}$$

where

$$\mathbf{F}(x)=\begin{pmatrix} f_1(x)\\ f_2(x)\\ \vdots\\ f_r(x)\end{pmatrix},\qquad \mathbf{G}(x)=\begin{pmatrix} g_1(x)\\ g_2(x)\\ \vdots\\ g_r(x)\end{pmatrix},\qquad \Theta=\begin{pmatrix}\theta_1\\ \theta_2\\ \vdots\\ \theta_r\end{pmatrix},$$

$$\mathbf{A}_i=\begin{pmatrix}\gamma_{1,1,i}&\gamma_{1,2,i}&\cdots&\gamma_{1,r,i}\\ \gamma_{2,1,i}&\gamma_{2,2,i}&\cdots&\gamma_{2,r,i}\\ \vdots&\vdots&\ddots&\vdots\\ \gamma_{r,1,i}&\gamma_{r,2,i}&\cdots&\gamma_{r,r,i}\end{pmatrix},\quad \mathbf{B}_i=\begin{pmatrix}\mu_{1,1,i}&\mu_{1,2,i}&\cdots&\mu_{1,r,i}\\ \mu_{2,1,i}&\mu_{2,2,i}&\cdots&\mu_{2,r,i}\\ \vdots&\vdots&\ddots&\vdots\\ \mu_{r,1,i}&\mu_{r,2,i}&\cdots&\mu_{r,r,i}\end{pmatrix},\quad \mathbf{C}_i=\begin{pmatrix}\nu_{1,1,i}&\nu_{1,2,i}&\cdots&\nu_{1,r,i}\\ \nu_{2,1,i}&\nu_{2,2,i}&\cdots&\nu_{2,r,i}\\ \vdots&\vdots&\ddots&\vdots\\ \nu_{r,1,i}&\nu_{r,2,i}&\cdots&\nu_{r,r,i}\end{pmatrix}.$$

Assume

$$\mathbf{F}_{\mathcal{L}}(x)=\mathfrak{F}_{\mathcal{L}}\mathfrak{S}_{\alpha,\mathcal{L}}(x),\qquad \mathbf{G}_{\mathcal{L}}(x)=\mathfrak{G}_{\mathcal{L}}\mathfrak{S}_{\alpha,\mathcal{L}}(x),\tag{5.3}$$

with

$$\mathfrak{F}_{\mathcal{L}}=\begin{pmatrix}\mathbf{f}_{1,0}&\mathbf{f}_{1,1}&\cdots&\mathbf{f}_{1,\mathcal{L}}\\ \mathbf{f}_{2,0}&\mathbf{f}_{2,1}&\cdots&\mathbf{f}_{2,\mathcal{L}}\\ \vdots&\vdots&\ddots&\vdots\\ \mathbf{f}_{r,0}&\mathbf{f}_{r,1}&\cdots&\mathbf{f}_{r,\mathcal{L}}\end{pmatrix},\quad \mathfrak{G}_{\mathcal{L}}=\begin{pmatrix}\mathbf{g}_{1,0}&\mathbf{g}_{1,1}&\cdots&\mathbf{g}_{1,\mathcal{L}}\\ \mathbf{g}_{2,0}&\mathbf{g}_{2,1}&\cdots&\mathbf{g}_{2,\mathcal{L}}\\ \vdots&\vdots&\ddots&\vdots\\ \mathbf{g}_{r,0}&\mathbf{g}_{r,1}&\cdots&\mathbf{g}_{r,\mathcal{L}}\end{pmatrix},$$

and $\mathbf{g}_{l,j}$ $(1\le l\le r,\ 0\le j\le\mathcal{L})$ can be given using the shifted Jacobi Gauss quadrature rule as follows:

$$\mathbf{g}_{l,j}=\frac{\alpha^{a+b+1}}{2^{a+b+1}h^{a,b}_{\alpha,i}}\sum_{i=0}^{\mathcal{L}}W_i^{(a+b)}S^{(a,b)}_{\alpha,i}\left(\frac{\alpha}{2}(x_i^{(a+b)}+1)\right)g_l\left(\frac{\alpha}{2}\left(x_i^{(a+b)}+1\right)\right),\qquad 1\le l\le r,$$

such that

$$\begin{cases} \dfrac{d\mathbf{F}_{\mathcal{L}}(x)}{dx}+\sum_{i=0}^{s}\mathbf{A}_i\mathbf{F}_{\mathcal{L}}(c_{i,l}x)=\mathbf{G}_{\mathcal{L}}(x)+\sum_{i=0}^{s}\int_0^{c_{i,l}x}\mathbf{B}_i\mathbf{F}_{\mathcal{L}}(w)dw+\int_0^x\mathbf{C}\,\mathbf{F}_{\mathcal{L}}(w)dw,\\ \mathbf{F}_{\mathcal{L}}(0)=\Theta,\end{cases}\tag{5.4}$$

We recall from (5.3) that

$$\frac{d\mathbf{F}_{\mathcal{L}}(x)}{dx}=\mathfrak{F}_{\mathcal{L}}\frac{d}{dx}\left(\mathfrak{S}_{\alpha,\mathcal{L}}(x)\right)=\mathfrak{F}_{\mathcal{L}}\mathbf{D}^{(1)}\mathfrak{S}_{\alpha,\mathcal{L}}(x),\qquad 1\le l\le r,\tag{5.5}$$

$$\mathbf{F}_{\mathcal{L}}(cx)=\mathfrak{F}_{\mathcal{L}}\mathfrak{S}_{\alpha,\mathcal{L}}(cx)=\mathfrak{F}_{\mathcal{L}}\mathbf{P}_c\mathfrak{S}_{\alpha,\mathcal{L}}(x),\qquad 1\le l\le r,\tag{5.6}$$

$$\int_0^x\mathbf{F}_{\mathcal{L}}(t)dt=\mathfrak{F}_{\mathcal{L}}\int_0^x\mathfrak{S}_{\alpha,\mathcal{L}}(t)dt=\mathfrak{F}_{\mathcal{L}}\mathbf{I}^{(1)}_{\mathcal{L}}\mathfrak{S}_{\alpha,\mathcal{L}}(x),\qquad 1\le l\le r,\tag{5.7}$$

$$\int_0^{c_{i,l}x} \mathbf{F}_{\mathcal{L}}(t)dt = \mathfrak{F}_{\mathcal{L}} \int_0^{c_{i,l}x} \mathfrak{S}_{\alpha,\mathcal{L}}(t)dt = \mathfrak{F}_{\mathcal{L}} \mathbf{I}_{\mathcal{L}}^{(1)} \mathbf{P}_{c_{i,l}} \mathfrak{S}_{\alpha,\mathcal{L}}(x), \qquad 1 \leq l \leq r. \tag{5.8}$$

It follows from (5.4)–(5.8) that

$$\mathfrak{F}_{\mathcal{L}}\mathbf{D}^{(1)}\mathfrak{S}_{\alpha,\mathcal{L}}(x) + \sum_{i=0}^{s} \mathbf{A}_i \mathfrak{F}_{\mathcal{L}} \mathbf{P}_{c_{i,l}} \mathfrak{S}_{\alpha,\mathcal{L}}(x) = \mathfrak{G}_{\mathcal{L}} \mathfrak{S}_{\alpha,\mathcal{L}}(x) + \sum_{i=0}^{s} \mathbf{B}_i \mathfrak{F}_{\mathcal{L}} \mathbf{I}_{\mathcal{L}}^{(1)} \mathbf{P}_{c_{i,l}} \mathfrak{S}_{\alpha,\mathcal{L}}(x) + \mathbf{C}\, \mathfrak{F}_{\mathcal{L}} \mathbf{I}_{\mathcal{L}}^{(1)} \mathfrak{S}_{\alpha,\mathcal{L}}(x),$$

and the residual of (5.4) can be given by

$$\mathbf{R}(x) = \mathfrak{F}_{\mathcal{L}}\mathbf{D}^{(1)}\mathfrak{S}_{\alpha,\mathcal{L}}(x) + \sum_{i=0}^{s} \mathbf{A}_i \mathfrak{F}_{\mathcal{L}} \mathbf{P}_{c_{i,l}} \mathfrak{S}_{\alpha,\mathcal{L}}(x) - \sum_{i=0}^{s} \mathbf{B}_i \mathfrak{F}_{\mathcal{L}} \mathbf{I}_{\mathcal{L}}^{(1)} \mathbf{P}_{c_{i,l}} \mathfrak{S}_{\alpha,\mathcal{L}}(x) - \mathbf{C}\, \mathfrak{F}_{\mathcal{L}} \mathbf{I}_{\mathcal{L}}^{(1)} \mathfrak{S}_{\alpha,\mathcal{L}}(x) - \mathfrak{G}_{\mathcal{L}} \mathfrak{S}_{\alpha,\mathcal{L}}(x),$$

where

$$\mathbf{R}(x) = [\mathcal{R}_{l,\mathcal{L}}, \mathcal{R}_{2,\mathcal{L}}, \cdots, \mathcal{R}_{r,\mathcal{L}}]^T.$$

Application of the spectral tau approach gives a system of $r(\mathcal{L}+1)$ algebraic equations as follows:

$$\begin{cases} \int_0^{\alpha} \mathcal{R}_{l,\mathcal{L}}(t) w_{\alpha}^{(a,b)} \mathcal{S}_{\alpha,0}^{(a,b)}(t)dt = 0, & l = 1, 2, \cdots, r, \\ \int_0^{\alpha} \mathcal{R}_{l,\mathcal{L}}(t) w_{\alpha}^{(a,b)} \mathcal{S}_{\alpha,1}^{(a,b)}(t)dt = 0, & l = 1, 2, \cdots, r, \\ \qquad \vdots \\ \int_0^{\alpha} \mathcal{R}_{l,\mathcal{L}}(t) w_{\alpha}^{(a,b)} \mathcal{S}_{\alpha,\mathcal{L}-1}^{(a,b)}(t)dt = 0, & l = 1, 2, \cdots, r, \\ \mathfrak{F}_{\mathcal{L}}^T \mathfrak{S}_{\alpha,\mathcal{L}}(0) = \theta_l, & l = 1, 2, \cdots, r. \end{cases} \tag{5.9}$$

Using (3.13), the system (5.9) can be simplified as follows:

$$\mathfrak{F}_{\mathcal{L}}\mathbf{D}^{(1)}{}_{\alpha}\mathbf{O}_{\mathcal{L}}^{i} + \sum_{i=0}^{s} \mathbf{A}_i \mathfrak{F}_{\mathcal{L}} \mathbf{P}_{c_{i,l}\alpha} \mathbf{O}_{\mathcal{L}}^{i} - \sum_{i=0}^{s} \mathbf{B}_i \mathfrak{F}_{\mathcal{L}} \mathbf{I}_{\mathcal{L}}^{(1)} \mathbf{P}_{c_{i,l}\alpha} \mathbf{O}_{\mathcal{L}}^{i} - \mathbf{C}\, \mathfrak{F}_{\mathcal{L}} \mathbf{I}_{\mathcal{L}}^{(1)}{}_{\alpha}\mathbf{O}_{\mathcal{L}}^{i} - \mathfrak{G}_{\mathcal{L}\alpha} \mathbf{O}_{\mathcal{L}}^{i} = 0, \tag{5.10}$$

with $l = 1, 2, \cdots, r,\ i = 0, 1, \cdots, \mathcal{L}-1$.
We denote $M_i,\ i = 0, 1, \cdots, \mathcal{L}-1$, as

$$M_{l,i} = \left({}_{\alpha}\mathbf{O}_{\mathcal{L}}^{i}\right)^T \left(\mathbf{D}^{(1)}\right)^T + \sum_{i=0}^{s} \mathbf{A}_i \left({}_{\alpha}\mathbf{O}_{\mathcal{L}}^{i}\right)^T \left(\mathbf{P}_{c_{i,l}}\right)^T - \sum_{i=0}^{s} \mathbf{B}_i \left({}_{\alpha}\mathbf{O}_{\mathcal{L}}^{i}\right)^T \left(\mathbf{P}_{c_{i,l}}\right)^T \left(\mathbf{I}_{\mathcal{L}}^{(1)}\right)^T - \mathbf{C}\, \left({}_{\alpha}\mathbf{O}_{\mathcal{L}}^{i}\right)^T \left(\mathbf{I}_{\mathcal{L}}^{(1)}\right)^T,$$

in which case the solution of (5.1) is reduced to the system

$$\mathbf{E}_l \mathfrak{F}_{\mathcal{L}}^T = \mathbf{R}_l, \qquad l = 1, 2, \cdots, r,$$

where

$$\mathbf{E}_l = \left[M_{l,0},\ M_{l,1},\ \cdots,\ M_{l,\mathcal{L}-1},\ C\right], \qquad l = 1, 2, \cdots, r,$$

$$\mathbf{R}_l = \left[\frac{g_{l,0}}{h_{\alpha,0}^{(a,b)}},\ \frac{g_{l,1}}{h_{1}^{(a,b)}},\ \frac{g_{l,2}}{h_{\alpha,2}^{(a,b)}},\ \cdots,\ \frac{g_{l,\mathcal{L}-1}}{h_{\alpha,\mathcal{L}-1}^{(a,b)}},\ \theta_l\right]^T, \qquad l = 1, 2, \cdots, r.$$

6. Two-dimensional case

The current section extends the application of the numerical approach to solve the two-dimensional multi-pantograph integro-differential equation as follows:

$$\begin{aligned}\frac{\partial^2 f(x,y)}{\partial x\partial y} + \sum_{i=0}^{s}\sum_{j=0}^{q}\gamma_{i,j} f(c_i x, d_j y) = g(x,y) + \int_0^y\int_0^x \mu_{i,j} f(t,u)dtdu\\ + \sum_{i=0}^{s}\sum_{j=0}^{q}\int_0^{c_i x}\int_0^{d_j y}\nu_{i,j} f(t,u)dtdu,\end{aligned} \tag{6.1}$$

with $f(0,y)=\theta(y)$ and $f(x,0)=\vartheta(x)$, where $\gamma_{i,j},\ \mu_{i,j},\ \nu_{i,j},\ c_j,\ d_j$; $(0\le i\le s, 0\le j\le q)$ are known real numbers.
In this regard, we have to find $f_{\mathcal{L},\mathcal{M}}\in\mathcal{S}^{\alpha}_{\mathcal{L}}\times\mathcal{S}^{\beta}_{\mathcal{M}}$, such that

$$\begin{aligned}\frac{\partial^2 f_{\mathcal{L},\mathcal{M}}(x,y)}{\partial x\partial y} + \sum_{i=0}^{s}\sum_{j=0}^{q}\gamma_{i,j} f_{\mathcal{L},\mathcal{M}}(c_i x, d_j y) = g_{\mathcal{L},\mathcal{M}}(x,y) + \int_0^y\int_0^x \mu_{i,j} f_{\mathcal{L},\mathcal{M}}(t,u)dtdu\\ + \sum_{i=0}^{s}\sum_{j=0}^{q}\int_0^{c_i x}\int_0^{d_j y}\nu_{i,j} f_{\mathcal{L},\mathcal{M}}(t,u)dtdu.\end{aligned} \tag{6.2}$$

Suppose that

$$\begin{aligned} f_{\mathcal{L},\mathcal{M}}(x,y) &= \mathcal{F}^T_{\mathcal{L},\mathcal{M}}\mathfrak{S}^{\alpha,\beta}_{\mathcal{L},\mathcal{M}}(x,y),\\ g_{\mathcal{L},\mathcal{M}}(x,y) &= \mathcal{G}^T_{\mathcal{L},\mathcal{M}}\mathfrak{S}^{\alpha,\beta}_{\mathcal{L},\mathcal{M}}(x,y),\end{aligned} \tag{6.3}$$

where

$$\mathcal{G}_{\mathcal{L},\mathcal{M}} = \begin{pmatrix} g_{0,0}\\ g_{0,1}\\ \vdots\\ g_{0,\mathcal{M}}\\ g_{1,0}\\ \vdots\\ g_{\mathcal{L},\mathcal{M}}\end{pmatrix};\qquad g_{l,m} = \frac{1}{h^{a,b}_{\alpha,l}h^{a,b}_{\beta,m}}\sum_{l=0}^{\mathcal{L}}\sum_{m=0}^{\mathcal{M}} W^{(a,b)}_{\mathcal{L},l,\alpha}W^{(a,b)}_{\mathcal{M},m,\beta}S^{(a,b)}_{\alpha,l}\left(x^{(a,b)}_{\mathcal{L},l,\alpha}\right)S^{(a,b)}_{\beta,m}\left(x^{(a,b)}_{\mathcal{L},l,\alpha}\right)g\left(x^{(a,b)}_{\mathcal{L},l,\alpha}, x^{(a,b)}_{\mathcal{M},m,\beta}\right).$$

Theorem 2. *Assume $\mathbb{I}_{\mathcal{L}}$ and $\mathbb{I}_{\mathcal{M}}$ are the identity matrices of orders $\mathcal{L}$ and $\mathcal{M}$, respectively, in which case*

$$\begin{aligned}\frac{\partial^2}{\partial x\partial y}\mathfrak{S}^{\alpha,\beta}_{\mathcal{L},\mathcal{M}}(x,y) &= \mathcal{D}^{(1)}_x\mathcal{D}^{(1)}_y\mathfrak{S}^{\alpha,\beta}_{\mathcal{L},\mathcal{M}}(x,y); && \mathcal{D}^{(1)}_x = \boldsymbol{D}^{(1)}_{\mathcal{L}}\otimes\mathbb{I}_{\mathcal{M}},\ \mathcal{D}^{(1)}_y = \mathbb{I}_{\mathcal{L}}\otimes\boldsymbol{D}^{(1)}_{\mathcal{M}},\\ \int_0^y\int_0^x\mathfrak{S}^{\alpha,\beta}_{\mathcal{L},\mathcal{M}}(t,u)dtdu &= \mathcal{I}^{(1)}_x\mathcal{I}^{(1)}_y\mathfrak{S}^{\alpha,\beta}_{\mathcal{L},\mathcal{M}}(x,y); && \mathcal{I}^{(1)}_x = \boldsymbol{I}^{(1)}_{\mathcal{L}}\otimes\mathbb{I}_{\mathcal{M}},\ \mathcal{I}^{(1)}_y = \mathbb{I}_{\mathcal{L}}\otimes\boldsymbol{I}^{(1)}_{\mathcal{M}},\\ \mathfrak{S}^{\alpha,\beta}_{\mathcal{L},\mathcal{M}}(cx,dy) &= \mathcal{P}_{x,c}\mathcal{P}_{y,d}\mathfrak{S}^{\alpha,\beta}_{\mathcal{L},\mathcal{M}}(x,y); && \mathcal{P}_{x,c} = \boldsymbol{P}_{\mathcal{L},c}\otimes\mathbb{I}_{\mathcal{M}},\ \mathcal{P}_{y,d} = \mathbb{I}_{\mathcal{L}}\otimes\boldsymbol{P}_{\mathcal{M},d},\\ \int_0^{dy}\int_0^{cx}\mathfrak{S}^{\alpha,\beta}_{\mathcal{L},\mathcal{M}}(t,u)dtdu &= \mathcal{I}^{(1)}_x\mathcal{I}^{(1)}_y\mathcal{P}_{x,c}\mathcal{P}_{y,d}\mathfrak{S}^{\alpha,\beta}_{\mathcal{L},\mathcal{M}}(x,y).\end{aligned}$$

Using (6.3) and Theorem 3, we get

$$\begin{aligned} \frac{\partial^2}{\partial x \partial y} f_{\mathcal{L},\mathcal{M}}(x,y) &= \mathcal{F}^T_{\mathcal{L},\mathcal{M}} \mathcal{D}^{(1)}_x \mathcal{D}^{(1)}_y \mathfrak{S}^{\alpha,\beta}_{\mathcal{L},\mathcal{M}}(x,y), \\ \int_0^y \int_0^x f_{\mathcal{L},\mathcal{M}}(t,u)dtdu &= \mathcal{F}^T_{\mathcal{L},\mathcal{M}} \mathcal{I}^{(1)}_x \mathcal{I}^{(1)}_y \mathfrak{S}^{\alpha,\beta}_{\mathcal{L},\mathcal{M}}(x,y), \\ f_{\mathcal{L},\mathcal{M}}(cx,dy) &= \mathcal{F}^T_{\mathcal{L},\mathcal{M}} \mathcal{P}_{x,c} \mathcal{P}_{y,d} \mathfrak{S}^{\alpha,\beta}_{\mathcal{L},\mathcal{M}}(x,y), \\ \int_0^{dy} \int_0^{cx} f_{\mathcal{L},\mathcal{M}}(t,u)dtdu &= \mathcal{F}^T_{\mathcal{L},\mathcal{M}} \mathcal{I}^{(1)}_x \mathcal{I}^{(1)}_y \mathcal{P}_{x,c} \mathcal{P}_{y,d} \mathfrak{S}^{\alpha,\beta}_{\mathcal{L},\mathcal{M}}(x,y). \end{aligned} \tag{6.4}$$

Then, the residual of (6.1) can be given by

$$\begin{aligned} \mathcal{R}_{\mathcal{L},\mathcal{M}}(x,y) = {}& \mathcal{F}^T_{\mathcal{L},\mathcal{M}} \mathcal{D}^{(1)}_x \mathcal{D}^{(1)}_y \mathfrak{S}^{\alpha,\beta}_{\mathcal{L},\mathcal{M}}(x,y) + \sum_{i=0}^{s} \sum_{j=0}^{q} \gamma_{i,j} \mathcal{F}^T_{\mathcal{L},\mathcal{M}} \mathcal{P}_{x,c_i} \mathcal{P}_{y,d_j} \mathfrak{S}^{\alpha,\beta}_{\mathcal{L},\mathcal{M}}(x,y) - \mathcal{G}^T_{\mathcal{L},\mathcal{M}} \mathfrak{S}^{\alpha,\beta}_{\mathcal{L},\mathcal{M}}(x,y) \\ & - \mu_{i,j} \mathcal{F}^T_{\mathcal{L},\mathcal{M}} \mathcal{I}^{(1)}_x \mathcal{I}^{(1)}_y \mathfrak{S}^{\alpha,\beta}_{\mathcal{L},\mathcal{M}}(x,y) - \sum_{i=0}^{s} \sum_{j=0}^{q} \nu_{i,j} \mathcal{F}^T_{\mathcal{L},\mathcal{M}} \mathcal{I}^{(1)}_x \mathcal{I}^{(1)}_y \mathcal{P}_{x,c_i} \mathcal{P}_{y,d_j} \mathfrak{S}^{\alpha,\beta}_{\mathcal{L},\mathcal{M}}(x,y). \end{aligned}$$

Finally, the following system of $(\mathcal{L}+1)(\mathcal{M}+1)$ is generated:

$$\int_0^{\alpha} \int_0^{\beta} \mathcal{R}_{\mathcal{L},\mathcal{M}}(x,y) \mathcal{S}^{(a,b)}_{\alpha,i}(x) \mathcal{S}^{(a,b)}_{\beta,j}(y) w^{(a,b)}_x(x) w^{(a,b)}_y(y) dydx = 0, \quad 0 \le i \le \mathcal{L}-1,\ 0 \le j \le \mathcal{M}-1, \tag{6.5}$$

$$\begin{aligned} \mathcal{F}^T_{\mathcal{L},\mathcal{M}} \mathfrak{S}^{\alpha,\beta}_{\mathcal{L},\mathcal{M}} \left(0, x^{(a,b)}_{\mathcal{M},j,\beta}\right) &= \theta\left(x^{(a,b)}_{\mathcal{M},j,\beta}\right), \qquad 0 \le j \le \mathcal{M}, \\ \mathcal{F}^T_{\mathcal{L},\mathcal{M}} \mathfrak{S}^{\alpha,\beta}_{\mathcal{L},\mathcal{M}} \left(x^{(a,b)}_{\mathcal{L},i,\alpha}, 0\right) &= \vartheta\left(x^{(a,b)}_{\mathcal{L},i,\alpha}\right), \qquad 0 \le i \le \mathcal{L}. \end{aligned} \tag{6.6}$$

Define the vector ${}_{\alpha,\beta}\mathbf{O}^{i,j}_{\mathcal{L},\mathcal{M}}$, $i = 0,1,\cdots,\mathcal{L}-1$, $j = 0,1,\cdots,\mathcal{M}-1$, as follows:

$${}_{\alpha,\beta}\mathbf{O}^{i,j}_{\mathcal{L},\mathcal{M}} = {}_{\alpha}\mathbf{O}^{i}_{\mathcal{L}} \otimes {}_{\beta}\mathbf{O}^{j}_{\mathcal{M}}, \quad i = 0,1,\cdots,\mathcal{L}-1,\ j = 0,1,\cdots,\mathcal{M}-1,$$

The system (6.5) is then simplified to

$$\begin{aligned} & \mathcal{F}^T_{\mathcal{L},\mathcal{M}} \mathcal{D}^{(1)}_x \mathcal{D}^{(1)}_y {}_{\alpha,\beta}\mathbf{O}^{i,j}_{\mathcal{L},\mathcal{M}} + \sum_{i=0}^{s} \sum_{j=0}^{q} \gamma_{i,j} \mathcal{F}^T_{\mathcal{L},\mathcal{M}} \mathcal{P}_{x,c_i} \mathcal{P}_{y,d_j} {}_{\alpha,\beta}\mathbf{O}^{i,j}_{\mathcal{L},\mathcal{M}} - \mathcal{G}^T_{\mathcal{L},\mathcal{M}} {}_{\alpha,\beta}\mathbf{O}^{i,j}_{\mathcal{L},\mathcal{M}} \\ & \qquad - \mu_{i,j} \mathcal{F}^T_{\mathcal{L},\mathcal{M}} \mathcal{I}^{(1)}_x \mathcal{I}^{(1)}_y {}_{\alpha,\beta}\mathbf{O}^{i,j}_{\mathcal{L},\mathcal{M}} - \sum_{i=0}^{s} \sum_{j=0}^{q} \nu_{i,j} \mathcal{F}^T_{\mathcal{L},\mathcal{M}} \mathcal{I}^{(1)}_x \mathcal{I}^{(1)}_y \mathcal{P}_{x,c_i} \mathcal{P}_{y,d_j} {}_{\alpha,\beta}\mathbf{O}^{i,j}_{\mathcal{L},\mathcal{M}}. \end{aligned}$$

We write $M_{i,j}$, $i = 0,1,\cdots,\mathcal{L}-1$, $j = 0,1,\cdots,\mathcal{M}-1$, as follows

$$\begin{aligned} M_{i,j} = {}& \left({}_{\alpha,\beta}\mathbf{O}^{i,j}_{\mathcal{L},\mathcal{M}}\right)^T \left(\mathcal{D}^{(1)}_y\right)^T \left(\mathcal{D}^{(1)}_x\right)^T + \sum_{i=0}^{s} \sum_{j=0}^{q} \gamma_{i,j} \left({}_{\alpha,\beta}\mathbf{O}^{i,j}_{\mathcal{L},\mathcal{M}}\right)^T \left(\mathcal{P}_{y,d_j}\right)^T \left(\mathcal{P}_{x,c_i}\right)^T \\ & - \mu_{i,j} \left({}_{\alpha,\beta}\mathbf{O}^{i,j}_{\mathcal{L},\mathcal{M}}\right)^T \left(\mathcal{I}^{(1)}_y\right)^T \left(\mathcal{I}^{(1)}_x\right)^T - \sum_{i=0}^{s} \sum_{j=0}^{q} \nu_{i,j} \left({}_{\alpha,\beta}\mathbf{O}^{i,j}_{\mathcal{L},\mathcal{M}}\right)^T \left(\mathcal{P}_{y,d_j}\right)^T \left(\mathcal{P}_{x,c_i}\right)^T \left(\mathcal{I}^{(1)}_y\right)^T \left(\mathcal{I}^{(1)}_x\right)^T, \end{aligned}$$

and

$$C_{1,j} = \left(\mathfrak{S}^{\alpha,\beta}_{\mathcal{L},\mathcal{M}}(0, y_j)\right)^T, \qquad j = 0, 1, \cdots, \mathcal{M},$$
$$C_{2,j} = \left(\mathfrak{S}^{\alpha,\beta}_{\mathcal{L},\mathcal{M}}(x_j, 0)\right)^T, \qquad j = 1, 2, \cdots, \mathcal{M}.$$

The solution of (6.1) is reduced to the system

$$\mathbf{E}F_{\mathcal{L},\mathcal{M}} = \mathbf{R},$$

where

$$\mathbf{E} = \left[M_{0,0},\ M_{0,1},\ \cdots,\ M_{0,\mathcal{M}-1},\ M_{1,0},\ \cdots,\ M_{\mathcal{L}-1,\mathcal{M}-1},\ C_{1,0},\ C_{1,1},\ \cdots,\ C_{1,\mathcal{M}},\ C_{2,1},\ C_{2,2},\ \cdots,\ C_{2,\mathcal{L}}\right],$$
$$\mathbf{R} = \left[\frac{g_{0,0}}{h^{(a,b)}_{\alpha,0}h^{(a,b)}_{\beta,0}},\ \frac{g_{0,1}}{h^{(a,b)}_{\alpha,0}h^{(a,b)}_{\beta,1}},\ \cdots,\ \frac{g_{\mathcal{L}-1,\mathcal{M}-1}}{h^{(a,b)}_{\alpha,\mathcal{L}-1}h^{(a,b)}_{\beta,\mathcal{M}-1}}, a_1(y_0), a_1(y_1),\ \cdots,\ a_1(y_{\mathcal{M}}),\ a_2(x_1), a_2(x_2), \cdots,\ a_2(x_{\mathcal{L}})\right]^T.$$

7. Convergence analysis

This section estimates the error achieved using the numerical approach proposed in Sections 3 and 6 for the one- and two-dimensional multi-pantograph integro-differential Eqs (3.1) and (6.1), respectively.

7.1. One-dimensional case

7.1.1. Error bound

This subsection is devoted to obtaining the error bound resulting from applying a numerical scheme based on shifted Jacobi polynomials to approximate any function $f(x)$ on $[0, \alpha]$.

Theorem 3. *Assume that $f_{\mathcal{L}}(x)$ is the best approximation of the function $f(x)$ achieved in terms of $\mathcal{S}^{(a,b)}_{\alpha,j}(x),\ 0 \le j \le \mathcal{L} + 1$, and $C = \max_{x\in(0,\alpha)} \left|\frac{\partial^{\mathcal{L}+1} f(x)}{\partial x^{\mathcal{L}+1}}\right|$. We then have*

$$\|f(x) - f_{\mathcal{L}}(x)\|_\infty \le C \frac{\alpha^{\mathcal{L}+1}\Gamma(\mathcal{L} + a + b + 1)\Gamma(\mathcal{L} + a + 2)}{2(\mathcal{L} + 1)\Gamma(2\mathcal{L} + a + b + 1)(\mathcal{L} + 1)!\Gamma(a + 1)}. \tag{7.1}$$

Proof. We begin the proof by using the definition of best approximation, which is

$$\|f(x) - f_{\mathcal{L}}(x)\|_\infty \le \|f(x) - \bar{f}_{\mathcal{L}}(x)\|_\infty, \qquad \forall \bar{f}_{\mathcal{L}}(x) \in \mathcal{S}^{\alpha}_{\mathcal{L}}. \tag{7.2}$$

We also use $\bar{f}_{\mathcal{L}}(x)$ to denote the interpolating polynomials of $f(x)$ at $x^{(a,b)}_{\mathcal{L},i,\alpha},\ 0 \le i \le \mathcal{L}$, as the roots of $\mathcal{S}^{(a,b)}_{\alpha,\mathcal{L}+1}(x)$, yielding

$$f(x) - \bar{f}_{\mathcal{L}}(x) = \frac{1}{(\mathcal{L} + 1)!} \frac{\partial^{\mathcal{L}+1} f(t)}{\partial x^{\mathcal{L}+1}} \prod_{i=0}^{\mathcal{L}} (x - x^{(a,b)}_{\mathcal{L},i,\alpha}), \qquad t \in [0, \alpha], \tag{7.3}$$

which implies

$$\|f(x) - \bar{f}_{\mathcal{L}}(x)\|_\infty \le \max \left|\frac{\partial^{\mathcal{L}+1} f(\varrho)}{\partial x^{\mathcal{L}+1}}\right| \frac{\left\|\prod_{i=0}^{\mathcal{L}}(x - x^{(a,b)}_{\mathcal{L},i,\alpha})\right\|_\infty}{(\mathcal{L} + 1)!}, \qquad \varrho \in [0, \alpha]. \tag{7.4}$$

Introducing the variable $\bar{x}$, where $\bar{x} = \frac{2}{\alpha}(x - \frac{\alpha}{2})$ and $\bar{x}^{(a,b)}_{\mathcal{L},i,\alpha}$, and the roots of $\mathcal{S}^{(a,b)}_{\alpha,\mathcal{L}+1}(\bar{x})$, such that $\bar{x}^{(a,b)}_{\mathcal{L},i,\alpha} = \frac{2}{\alpha}(x^{(a,b)}_{\mathcal{L},i,\alpha} - \frac{\alpha}{2})$, $0 \le i \le \mathcal{L}$, we get

$$\begin{aligned}
\max_{0\le x, x^{(a,b)}_{\mathcal{L},i,\alpha}\le\alpha} \left|\prod_{i=0}^{\mathcal{L}}(x - x^{(a,b)}_{\mathcal{L},i,\alpha})\right| &= \max_{-1\le\bar{x},\bar{x}^{(a,b)}_{\mathcal{L},i,\alpha}\le 1} \left|\prod_{i=0}^{\mathcal{L}}\frac{\alpha}{2}(\bar{x} - \bar{x}^{(a,b)}_{\mathcal{L},i,\alpha})\right| \\
&= \left(\frac{\alpha}{2}\right)^{\mathcal{L}+1} \max_{-1\le\bar{x},\bar{x}^{(a,b)}_{\mathcal{L},i,\alpha}\le 1} \left|\prod_{i=0}^{\mathcal{L}}(\bar{x} - \bar{x}^{(a,b)}_{\mathcal{L},i,\alpha})\right| \\
&= \left(\frac{\alpha}{2}\right)^{\mathcal{L}+1} \max_{-1\le\bar{x},\bar{x}^{(a,b)}_{\mathcal{L},i,\alpha}\le 1} \left|\frac{2^{\mathcal{L}}\mathcal{L}!\Gamma(\mathcal{L}+a+b+1)\mathcal{S}^{(a,b)}_{\alpha,\mathcal{L}+1}(x)}{\Gamma(2\mathcal{L}+a+b+1)}\right| \\
&= \frac{\alpha^{\mathcal{L}+1}\mathcal{L}!\Gamma(\mathcal{L}+a+b+1)}{2\Gamma(2\mathcal{L}+a+b+1)} \max_{-1\le\bar{x},\bar{x}^{(a,b)}_{\mathcal{L},i,\alpha}\le 1} \left|\mathcal{S}^{(a,b)}_{\alpha,\mathcal{L}+1}(x)\right|.
\end{aligned} \tag{7.5}$$

Additionally, one can write

$$\max_{-1\le\bar{x},\bar{x}^{(a,b)}_{\mathcal{L},i,\alpha}\le 1} \left|\mathcal{S}^{(a,b)}_{\alpha,\mathcal{L}+1}(x)\right| = \mathcal{S}^{(a,b)}_{\alpha,\mathcal{L}+1}(1) = \frac{\Gamma(\mathcal{L}+a+2)}{(\mathcal{L}+1)!\Gamma(a+1)}. \tag{7.6}$$

Thanks to (7.2)–(7.6), it is clear that

$$\|f(x) - f_{\mathcal{L}}(x)\|_\infty \le C\frac{\alpha^{\mathcal{L}+1}\Gamma(\mathcal{L}+a+b+1)\Gamma(\mathcal{L}+a+2)}{2(\mathcal{L}+1)\Gamma(2\mathcal{L}+a+b+1)(\mathcal{L}+1)!\Gamma(a+1)}. \tag{7.7}$$

At this stage, a bound on the absolute error between $f(x)$ and $f_{\mathcal{L}}(x)$ is given, based on shifted Jacobi polynomials. □

7.1.2. Error estimation and residual correction

The current subsection is devoted to estimate the error achieved using the numerical scheme introduced in Section 3 with the residual error function. In this regard, we define the error function $E_{\mathcal{L}}(x) = f(x) - f_{\mathcal{L}}(x)$, where $f(x)$ ıs the exact solution for the multi-pantograph integro-differential Eq (3.1) and $f_{\mathcal{L}}(x)$ is its numerical solution. We then have

$$\frac{d}{dx}f_{\mathcal{L}}(x) + \sum_{i=0}^{s}\gamma_i f_{\mathcal{L}}(c_i x) = g_{\mathcal{L}}(x) + \sum_{i=0}^{s}\int_0^{c_i x}\mu_i f_{\mathcal{L}}(t)dt + \int_0^x \nu f_{\mathcal{L}}(t)dt + \mathcal{R}_{\mathcal{L}}(x), \tag{7.8}$$

where $f_{\mathcal{L}}(0) = \theta$, and $\mathcal{R}_{\mathcal{L}}(x)$ is the residual function defined in (3.11).
Subtracting (7.12) from (3.1), we have

$$\frac{d}{dx}E_{\mathcal{L}}(x) + \sum_{i=0}^{s}\gamma_i E_{\mathcal{L}}(c_i x) = g(x) - g_{\mathcal{L}}(x) + \sum_{i=0}^{s}\int_0^{c_i x}\mu_i E_{\mathcal{L}}(t)dt + \int_0^x \nu E_{\mathcal{L}}(t)dt - \mathcal{R}_{\mathcal{L}}(x), \tag{7.9}$$

with $E_{\mathcal{L}}(0) = 0$.
We now solve (7.9) using the numerical technique introduced in Section 3 by approximating $E_{\mathcal{L}}(x)$ as

$$E_{\mathcal{L},\mathcal{U}}(x) = \mathcal{E}^T_{\mathcal{U}}\Im_{\alpha,\mathcal{U}}(x). \tag{7.10}$$

Finally, it is clear that an estimate of the absolute error function $|E_{\mathcal{L}}(x)| = |f(x) - f_{\mathcal{L}}(x)|$ can be obtained using the absolute error function $|E_{\mathcal{L},\mathcal{U}}(x)|$.

7.2. Two-dimensional case

7.2.1. Error bound

Here, we obtain the error bound of a numerical scheme based on shifted Jacobi polynomials to approximate any function $f(x,y)$ in $[0,\alpha]\times[0,\beta]$.

Theorem 4. *Assume that $f_{\mathcal{L},\mathcal{M}}(x,y)$ is the best approximation of the function $f(x,y)$ achieved in terms of $\mathcal{S}^{(a,b)}_{\alpha,j}(x)\mathcal{S}^{(a,b)}_{\beta,k}(y)$, $0\leq j\leq \mathcal{L}+1$, $0\leq k\leq \mathcal{M}+1$, $C_1=\max_{(x,y)\in(0,\alpha)\times(0,\beta)}\left|\frac{\partial^{\mathcal{L}+1}f(x,y)}{\partial x^{\mathcal{L}+1}}\right|$, $C_2=\max_{(x,y)\in(0,\alpha)\times(0,\beta)}\left|\frac{\partial^{\mathcal{M}+1}f(x,y)}{\partial y^{\mathcal{M}+1}}\right|$, and $C_3=\max_{(x,y)\in(0,\alpha)\times(0,\beta)}\left|\frac{\partial^{\mathcal{L}+\mathcal{M}+2}f(x,y)}{\partial x^{\mathcal{L}+1}y^{\mathcal{M}+1}}\right|$. We then have*

$$
\begin{aligned}
\|f(x,y)-f_{\mathcal{L},\mathcal{M}}(x,y)\|_\infty \leq{}& C_1\frac{\alpha^{\mathcal{L}+1}\Gamma(\mathcal{L}+a+b+1)\Gamma(\mathcal{L}+a+2)}{2(\mathcal{L}+1)\Gamma(2\mathcal{L}+a+b+1)(\mathcal{L}+1)!\Gamma(a+1)}\\
&+C_2\frac{\alpha^{\mathcal{L}+1}\beta^{\mathcal{M}+1}\Gamma(\mathcal{L}+a+b+1)\Gamma(\mathcal{M}+a+b+1)\Gamma(\mathcal{L}+a+2)\Gamma(\mathcal{M}+a+2)}{2(\mathcal{L}+1)(\mathcal{M}+1)\Gamma(2\mathcal{L}+a+b+1)\Gamma(2\mathcal{M}+a+b+1)(\mathcal{L}+1)!(\mathcal{M}+1)!\Gamma^2(a+1)}\\
&+C_3\frac{\beta^{\mathcal{M}+1}\Gamma(\mathcal{M}+a+b+1)\Gamma(\mathcal{M}+a+2)}{2(\mathcal{M}+1)\Gamma(2\mathcal{M}+a+b+1)(\mathcal{M}+1)!\Gamma(a+1)}.
\end{aligned}
\tag{7.11}
$$

Proof. Following the same steps as performed in the proof of Theorem 7.1, we can complete the proof. □

7.2.2. Error estimation and residual correction

We now use the residual error function to estimate the error using the numerical approach discussed in Section 6. To do that, we assume $E_{\mathcal{L},\mathcal{M}}(x,y)=f(x,y)-f_{\mathcal{L},\mathcal{M}}(x,y)$, where $f(x,y)$ and $f_{\mathcal{L},\mathcal{M}}(x,y)$ are the exact and numerical solutions for the two-dimensional multi-pantograph integro-differential Eq (6.1). We can then write

$$
\begin{aligned}
\frac{\partial^2 f_{\mathcal{L},\mathcal{M}}(x,y)}{\partial x\partial y}+\sum_{i=0}^{s}\sum_{j=0}^{q}\gamma_{i,j}f_{\mathcal{L},\mathcal{M}}(c_ix,d_jy)={}&g_{\mathcal{L},\mathcal{M}}(x,y)+\int_0^y\int_0^x\mu_{i,j}f_{\mathcal{L},\mathcal{M}}(t,u)dtdu\\
&+\sum_{i=0}^{s}\sum_{j=0}^{q}\int_0^{c_ix}\int_0^{d_jy}\nu_{i,j}f_{\mathcal{L},\mathcal{M}}(t,u)dtdu+\mathcal{R}_{\mathcal{L},\mathcal{M}}(x,y),
\end{aligned}
\tag{7.12}
$$

with $f_{\mathcal{L},\mathcal{M}}(0,y)=\theta(y)$ and $f_{\mathcal{L},\mathcal{M}}(x,0)=\vartheta(x)$.
Now, if we subtract (7.12) from (6.1), we get

$$
\begin{aligned}
\frac{\partial^2 E_{\mathcal{L},\mathcal{M}}(x,y)}{\partial x\partial y}+\sum_{i=0}^{s}\sum_{j=0}^{q}\gamma_{i,j}E_{\mathcal{L},\mathcal{M}}(c_ix,d_jy)={}&g(x,y)-g_{\mathcal{L},\mathcal{M}}(x,y)+\int_0^y\int_0^x\mu_{i,j}E_{\mathcal{L},\mathcal{M}}(t,u)dtdu\\
&+\sum_{i=0}^{s}\sum_{j=0}^{q}\int_0^{c_ix}\int_0^{d_jy}\nu_{i,j}E_{\mathcal{L},\mathcal{M}}(t,u)dtdu-\mathcal{R}_{\mathcal{L},\mathcal{M}}(x,y),
\end{aligned}
$$

with $E_{\mathcal{L},\mathcal{M}}(0,y)=\theta(y)$ and $E_{\mathcal{L},\mathcal{M}}(x,0)=\vartheta(x)$.
Finally, if we apply the numerical scheme discussed in Section 6 using the approximation,

$$
E_{\mathcal{L},\mathcal{M},\mathcal{U},\mathcal{V}}(x,y)=\mathcal{E}^T_{\mathcal{U},\mathcal{V}}\mathfrak{S}^{\alpha,\beta}_{\mathcal{U},\mathcal{V}}(x,y),
\tag{7.13}
$$

we can estimate the absolute error function $|E_{\mathcal{L},\mathcal{M},\mathcal{U},\mathcal{V}}(x,y)|$.

8. Test problems

8.1. Convergence test

8.1.1. One-dimensional case

This subsection focuses on assessing the convergence behavior of the proposed numerical method. In this regard, we address the following problem:

$$\frac{df(x)}{dx} = f(x) + f(cx) + \int_0^x f(t)dt + \int_0^{cx} f(t)dt + \int_0^{(1-c)x} f(t)dt = g(x), \qquad 0 \le x \le 1, \qquad (8.1)$$

with $f(0) = 0$ and the exact solution is $f(x) = x^4 Log(1 + x) sin(x)$.

We apply the numerical scheme proposed in Section 3 to the current problem at $(a, b) = (5, 5)$ with different choices of c. We list the maximum absolute errors (MAEs) of the numerical solution $f_{\mathcal{L}}(x)$ in Table 1 at $c = \{0.3, 0.5, 0.9\}$ with $(a, b) = (5, 5)$. Moreover, in Figure 1, we plot the logarithmic function of MAEs (Log_{10} MAEs) of $f_{\mathcal{L}}(x)$ to show the convergence with various choices of $\mathcal{L}$.

The numerical results shown in Table 1 and Figure 1 confirm that the MAEs of the approximate solution decrease with increasing values of $\mathcal{L}$, ensuring the high convergence and accuracy of the considered approach.

Table 1. MAEs of $f_{\mathcal{L}}(x)$ with $(a, b) = (5, 5)$ for problem (8.5).

$\mathcal{L}$	$c = 0.3$	$c = 0.5$	$c = 0.9$
2	4.8849×10^{-1}	5.2859×10^{-1}	5.8873×10^{-1}
4	4.6081×10^{-2}	4.9906×10^{-2}	5.9441×10^{-2}
6	2.5070×10^{-3}	2.6675×10^{-3}	3.2643×10^{-3}
8	8.7892×10^{-6}	9.2539×10^{-6}	1.0771×10^{-5}
10	3.5186×10^{-7}	3.7064×10^{-7}	4.5861×10^{-7}
12	1.0734×10^{-8}	1.1277×10^{-8}	1.3894×10^{-8}
14	3.9307×10^{-10}	4.1211×10^{-10}	5.0415×10^{-10}
16	1.4284×10^{-11}	1.4954×10^{-11}	1.8199×10^{-11}
18	5.1736×10^{-13}	5.4090×10^{-13}	6.5569×10^{-13}
20	1.8762×10^{-14}	1.9872×10^{-14}	2.3647×10^{-14}
22	1.3981×10^{-15}	9.9920×10^{-16}	1.1102×10^{-15}

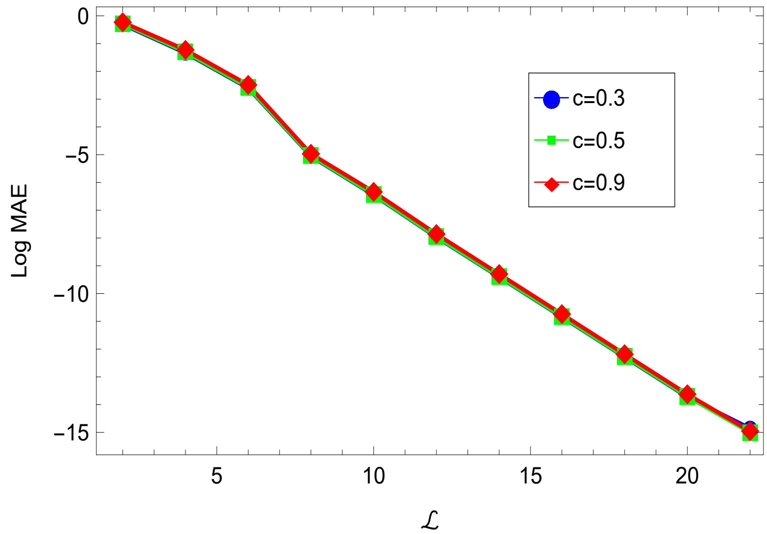

Figure 1. Convergence of $f_{\mathcal{L}}(x)$ at $(a, b) = (5, 5)$ for problem (8.5).

8.1.2. Two-dimensional case

To test the convergence of the numerical scheme discussed in Section 6, we consider the following problem:

$$\frac{\partial^2 f(x,y)}{\partial x \partial y} + f(x,y) - f(\frac{1}{4}x, \frac{1}{3}y) + \int_0^{\frac{1}{3}y} \int_0^{\frac{1}{4}x} f(t,s)dtds - \int_0^{y} \int_0^{x} f(t,s)dtds = g(x,y), \tag{8.2}$$

where $0 \leq x, y \leq 1$, $f(0, y) = 0$, $f(x, 0) = \log(1 + x)$, and $g(x, y)$ is chosen so that the exact solution is $f(x, y) = y \sin^2(x) + \log(1 + x)$. Table 2 lists the MAEs of $f(x, y)$ at $(a, b) = (0, 0)$ with $\mathcal{M} = 2$ and various choices of $\mathcal{L}$.

Table 2. MAEs of $f(x, y)$ for problem (8.2) at $(a, b) = (0, 0)$ with $\mathcal{M} = 2$.

$\mathcal{L}$	4	8	12	16	20	24
MAEs	2.150×10^{-3}	1.581×10^{-7}	5.827×10^{-11}	4.363×10^{-14}	7.771×10^{-16}	5.551×10^{-16}

8.2. Comparison test

8.2.1. One-dimensional case

The present subsection is devoted to confirming the superiority of the proposed numerical approach over other existing approaches. Therefore, we examine the following integro-differential equation [14, 21]:

$$\frac{df(x)}{dx} + \gamma_1 f(x) + \gamma_2 f(cx) + \mu \int_0^{x} f(t)dt + \nu \int_0^{cx} f(t)dt = g(x), \qquad 0 \leq x \leq \alpha, \tag{8.3}$$

with $f(0) = 0$ and the exact solution is $f(x) = 1 - e^{-x}$.

Zhao et al. [14] applied the BTS and LIC approaches to solve Problem (8.3) with $\gamma_1 = -3$, $\gamma_2 = 1$, $\mu = -4$, $\nu = 1$, $c = 0.5$, $\alpha = 1$, $\theta = 0$, and $g(x) = 1 - 3.5x$, while the authors in [21] used the CSCM to get its numerical solution with $\gamma_1 = 0,\ \gamma_2 = -1,\ \mu = -1,\ \nu = -1,\ c = 0.5,\ \alpha = 10,\ \theta = 0$, and $g(x) = 1-1.5x$. We applied the numerical method presented in Section 3 to solve (8.3) and compared the absolute errors (AEs) of $f_{\mathcal{L}}(x)$ at $(a, b) = (1, 1)$ with those given using the BTS and LIC approaches [14] in Table 3, and those at $(0, 0)$ with those given using the CSCM [21] in Table 4. Figure 2 plots the Log_{10} MAEs, AEs and the approximate solution of $f(x)$ at $\gamma_1 = -3,\ \gamma_2 = 1,\ \mu = -4,\ \nu = 1,\ c = 0.5,\ \alpha = 1,\ \theta = 0$, with $(a, b) = (2, 2)$ and $\mathcal{L} = 24$.

The numerical results shown in Tables 3 and 4 and Figure 2 indicate that the AEs of the numerical solution achieved using the proposed method are lower than those achieved using the BTS and LIC approaches [14] and the CSCM [21] at the same $\mathcal{L}$ values, which ensures the high accuracy and convergence of our numerical scheme compared with the BTS and LIC approaches [14] and the CSCM [21].

Table 3. AEs of $f(x)$ with $\gamma_1 = -3,\ \gamma_2 = 1,\ \mu = -4,\ \nu = 1,\ c = 0.5,\ \alpha = 1$, and $\theta = 0$ for problem (8.3).

	$\mathcal{L} = 3$	$\mathcal{L} = 6$	$\mathcal{L} = 8$	$\mathcal{L} = 10$	$\mathcal{L} = 12$
BTS [14] ($x = 0.5$)	2.401×10^{-4}	9.175×10^{-8}	2.573×10^{-10}	4.907×10^{-13}	5.551×10^{-16}
Our method ($x = 0.5$)	4.946×10^{-3}	1.611×10^{-7}	1.542×10^{-10}	9.580×10^{-14}	2.220×10^{-16}
	$\mathcal{L} = 2$	$\mathcal{L} = 4$	$\mathcal{L} = 6$	$\mathcal{L} = 8$	$\mathcal{L} = 10$
LIC [14] ($x = 1$)	5.200×10^{-3}	2.033×10^{-5}	3.540×10^{-8}	3.463×10^{-11}	2.986×10^{-14}
Our method ($x = 1$)	2.746×10^{-2}	1.620×10^{-5}	2.520×10^{-9}	2.044×10^{-12}	1.110×10^{-15}

Table 4. AEs of $f(x)$ with $\gamma_1 = 0,\ \gamma_2 = -1,\ \mu = -1,\ \nu = -1,\ c = 0.5,\ \alpha = 10$, and $\theta = 0$ for problem (8.3).

	CSCM [21]			Our method		
x	$\mathcal{L} = 16$	$\mathcal{L} = 20$	$\mathcal{L} = 24$	$\mathcal{L} = 16$	$\mathcal{L} = 20$	$\mathcal{L} = 24$
1	2.321×10^{-6}	6.569×10^{-8}	1.673×10^{-12}	5.760×10^{-9}	1.463×10^{-12}	1.110×10^{-16}
2	3.665×10^{-6}	8.041×10^{-8}	3.101×10^{-11}	2.000×10^{-8}	5.175×10^{-12}	4.163×10^{-16}
3	2.102×10^{-6}	8.005×10^{-8}	2.551×10^{-11}	6.206×10^{-8}	1.662×10^{-11}	1.769×10^{-15}
4	3.001×10^{-6}	7.561×10^{-8}	3.101×10^{-11}	1.861×10^{-7}	4.973×10^{-11}	5.818×10^{-15}
5	2.061×10^{-6}	8.021×10^{-8}	3.536×10^{-11}	5.359×10^{-7}	1.431×10^{-10}	1.727×10^{-14}
6	2.983×10^{-6}	8.553×10^{-8}	4.013×10^{-11}	1.509×10^{-6}	4.032×10^{-10}	4.910×10^{-14}
7	2.332×10^{-6}	1.479×10^{-7}	3.836×10^{-11}	4.197×10^{-6}	1.121×10^{-9}	1.369×10^{-13}
8	2.863×10^{-6}	7.350×10^{-8}	4.462×10^{-11}	1.156×10^{-5}	3.090×10^{-9}	3.778×10^{-13}
9	1.153×10^{-5}	8.102×10^{-8}	3.205×10^{-11}	3.172×10^{-5}	8.472×10^{-9}	1.036×10^{-12}

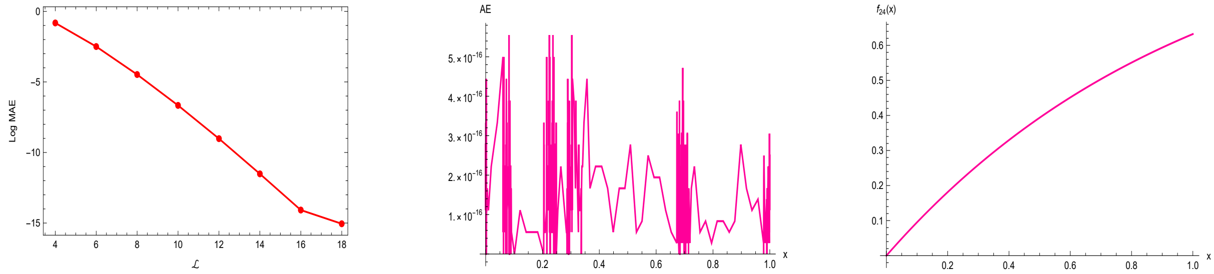

Figure 2. Log_{10} MAEs, AE, and approximate solutions of $f(x)$ for problem (8.3).

8.2.2. Two-dimensional case

To test the validity of the numerical approach for solving two-dimensional Volterra-type integro-differential equations, we consider the following problem:

$$\frac{\partial^2 f(x,y)}{\partial x \partial y} + f(x,y) - f(\frac{2}{3}x, \frac{1}{2}y) + \int_0^{\frac{1}{4}y}\int_0^{\frac{1}{4}x} f(t,s)dtds - \int_0^{y}\int_0^{x} f(t,s)dtds = g(x,y), \tag{8.4}$$

where $0 \leq x, y \leq 1$, $f(0,y) = f(x,0) = 0$, and $g(x,y)$ is chosen so that the exact solution is $f(x,y) = x^3(e^y - 1)$.

We apply the numerical scheme discussed in Section 6 to solve this problem with $\mathcal{L} = 4$ and various values of $\mathcal{M}$. Table 5 gives the AEs of $f(x,y)$ at $(a,b) = (2,2)$ and $\mathcal{M} = \{4, 8, 12, 16\}$. Figure 3 plots the AEs of $f(x,y)$ at $(\mathcal{L}, \mathcal{M}) = (4,16)$ and $(a,b) = (1,0)$. Figure 4 obtains the contour plots of the AEs of $f(x,y)$ at $(a,b) = (1,0)$ and various values of $\mathcal{L}$ and $\mathcal{M}$.

The results in Table 5 and Figures 3 and 4 confirm the high accuracy and convergence of the proposed numerical scheme when applied to a two-dimensional Volterra-type integro-differential equation.

Table 5. AEs of $f(x,y)$ for problem (8.4).

(x,y)	$\mathcal{M} = 4$	$\mathcal{M} = 8$	$\mathcal{M} = 12$	$\mathcal{M} = 16$
(0.1,0.1)	6.3085×10^{-3}	3.1577×10^{-7}	6.7570×10^{-13}	9.1200×10^{-16}
(0.2,0.2)	2.0864×10^{-2}	7.4917×10^{-7}	1.4439×10^{-12}	1.3810×10^{-15}
(0.3,0.3)	3.8636×10^{-2}	1.1806×10^{-6}	2.2253×10^{-12}	1.7590×10^{-15}
(0.4,0.4)	5.6723×10^{-2}	1.6389×10^{-6}	3.0490×10^{-12}	2.1718×10^{-15}
(0.5,0.5)	7.4414×10^{-2}	2.1158×10^{-6}	3.9319×10^{-12}	3.0253×10^{-15}
(0.6,0.6)	9.3176×10^{-2}	2.6376×10^{-6}	4.8913×10^{-12}	4.1078×10^{-15}
(0.7,0.7)	1.1656×10^{-1}	3.2346×10^{-6}	5.9539×10^{-12}	5.6066×10^{-15}
(0.8,0.8)	1.5008×10^{-1}	3.8594×10^{-6}	7.1522×10^{-12}	7.2164×10^{-15}
(0.9,0.9)	2.0097×10^{-1}	4.6940×10^{-6}	8.4501×10^{-11}	9.9920×10^{-15}

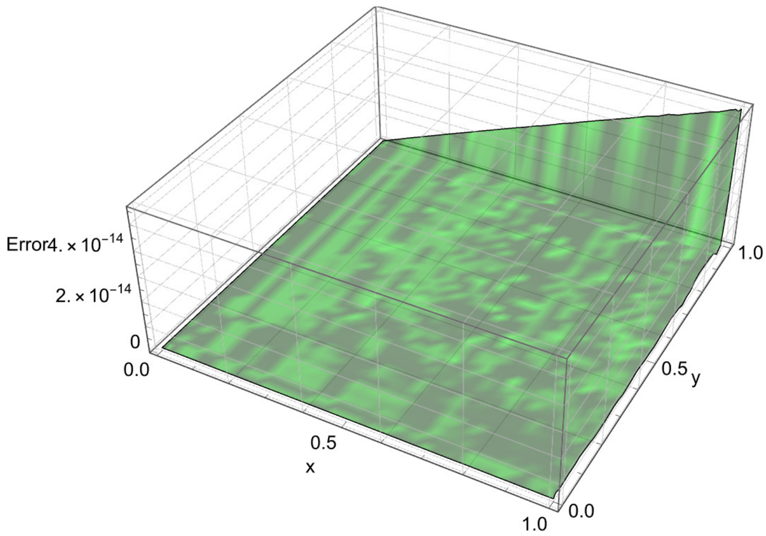

Figure 3. AEs of $f(x, y)$ at $(\mathcal{L}, \mathcal{M}) = (4, 16)$ with $(a, b) = (1, 0)$ for problem (8.4).

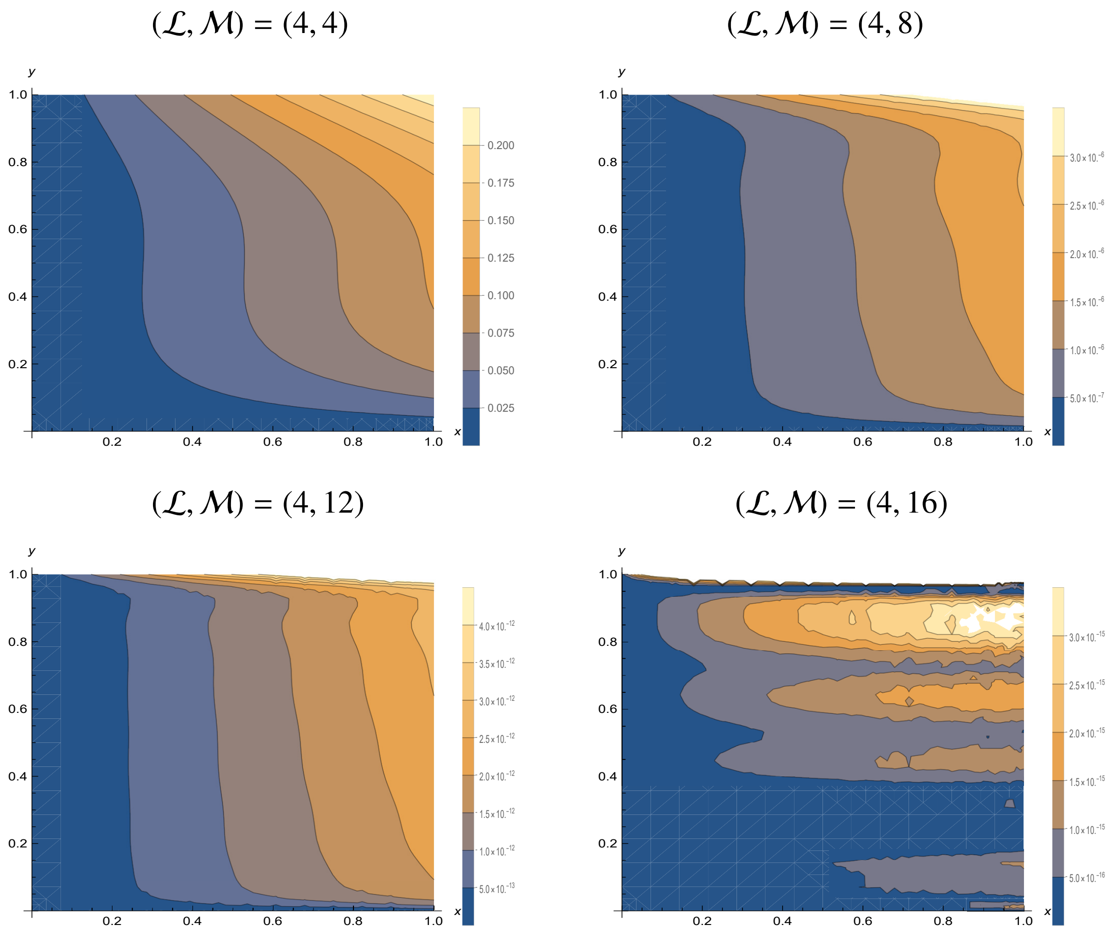

Figure 4. AEs of $f(x, y)$ at $(a, b) = (0, 1)$ for problem (8.4).

8.3. Equation with irregular solution

Here, we evaluate the reliability of the considered numerical approach discussed in Section 3 for a problem with an irregular solution. Consider the following

$$\frac{df(x)}{dx} - f(\frac{1}{2}x) - \int_0^x f(t)dt - \int_0^{\frac{1}{2}x} f(t)dt = \frac{5}{2}x^{\frac{3}{2}} - \frac{1}{4\sqrt{2}}x^{\frac{5}{2}} - \frac{2}{7}x^{\frac{7}{2}} - \frac{1}{28\sqrt{2}}x^{\frac{7}{2}}, \qquad 0 \leq x \leq 1, \quad (8.5)$$

with $f(0) = 0$, and the exact solution is $f(x) = x^{\frac{5}{2}}$. Table 6 lists the MAEs of $f(x)$ at $(a, b) = (2, 2)$ with various choices of $\mathcal{L}$.

Table 6. MAEs of $f(x)$ for problem (8.5) at $(a, b) = (2, 2)$.

$\mathcal{L}$	4	8	12	16	20	24
MAEs	4.750×10^{-3}	2.453×10^{-4}	4.321×10^{-5}	1.231×10^{-5}	4.577×10^{-6}	2.016×10^{-6}

8.4. Equation with variable kernel functions

This subsection tests the performance of the proposed numerical scheme for Volterra-type integro-differential equation with variable kernel functions, so we consider the following problem [21]:

$$\frac{df(x)}{dx} = \frac{1}{2}f(x) + f(\frac{1}{4}x) + \int_0^x e^{t+x} f(t)dt + \int_0^{\frac{1}{4}x} t^{\rho} f(t)dt = g(x), \qquad (8.6)$$

with $f(0) = 0$ and where the exact solution is $f(x) = e^x - 1$.

To obtain the numerical solution of the current problem at $\rho = 1$, Zhao et al. [11] applied the Sinc collocation method (SCM), and Ji et al. [21] applied the CSCM. Table 7 lists the MAEs of $f_{\mathcal{L}}(x)$ at $(a, b) = (0.5, 0.5)$ and various choices of $\mathcal{L} = \{4, 8, 12, 16\}$, and compares them with those given by the SCM [11] with $N = \{4, 8, 12, 16\}$ and CSCM [21] with $N = \{10, 20, 30, 40\}$.

The numerical results shown in Table 7 confirm that the proposed numerical scheme is a good choice for dealing with Volterra-type integro-differential equations with variable kernel functions and is more accurate than SCM [11] and CSCM [21].

Table 7. Comparing the MAEs of $f(x)$ versus the SCM [11] and CSCM [21] for problem (8.6) at $\rho = 1$.

SCM [11]		CSCM [21]		Present scheme	
N	MAE	N	MAE	$\mathcal{L}$	MAE
10	2.2328×10^{-4}	4	8.1760×10^{-4}	4	9.4465×10^{-5}
20	5.7215×10^{-6}	8	7.7913×10^{-9}	8	2.3189×10^{-9}
30	2.8939×10^{-7}	12	2.8315×10^{-14}	12	7.9621×10^{-15}
40	2.2096×10^{-7}	16	3.3316×10^{-16}	16	6.0704×10^{-16}

Remark 1. *To verify the applicability of the proposed numerical scheme to a weakly singular kernel Volterra integro-differential equation, we test the numerical approach presented in Section 4 to problem* (8.6) *at* $\rho = -0.5$. *In Table 8, we list the MAEs of* $f(x)$ *with* $(a, b) = (0, 0)$ *and* $\mathcal{L} = \{4, 8, 12, 16, 20\}$.

The MAEs shown in Table 8 are not as good as those shown in Table 7, nor is the convergence rate, indicating that the proposed numerical scheme is not optimal for handling weakly singular kernel Volterra integro-differential equations. However, the numerical scheme presented here can be modified to suit this case by using a graded mesh or by considering another basis function that is not generally smooth, such as a generalized Jacobi function.

Table 8. MAEs of $f(x)$ for problem (8.6) at $\rho = -0.5$.

$\mathcal{L}$	4	8	12	16	20
MAEs	1.8591×10^{-3}	3.3511×10^{-4}	1.1046×10^{-4}	4.9910×10^{-5}	2.6622×10^{-5}

8.5. System of equations

Here, we test the accuracy and convergence of the proposed numerical scheme when applied to a system of Volterra-type integro-differential equations. Consider the following problem:

$$\begin{cases} f_1^{(1)}(x) = f_1(x) + f_3(x) + f_2(\tfrac{1}{2}x) + \int_0^x f_3(t)dt + \int_0^{\frac{1}{2}x} f_1(t)dt \\ f_2^{(1)}(x) = f_1(x) + f_2(x) + f_1(\tfrac{1}{2}x) + f_2(\tfrac{1}{2}x) + \int_0^x f_3(t)dt + \int_0^{\frac{1}{2}x} f_2(t)dt - \int_0^{\frac{1}{2}x} f_3(t)dt, \\ f_3^{(1)}(x) = f_2(x) + f_3(x) + f_1(\tfrac{1}{2}x) + f_3(\tfrac{1}{2}x) + \int_0^x f_2(t)dt + \int_0^{\frac{1}{2}x} f_2(t)dt - \int_0^{\frac{1}{2}x} f_3(t)dt, \\ f_1(0) = 1, \quad f_2(0) = 0, \quad f_3(0) = 0, \quad 0 \le x \le 1. \end{cases} \tag{8.7}$$

with an exact solution $f_1(x) = e^x$, $f_2(x) = \log(x+1)$, and $f_4(x) = x^4$.

Table 9 shows the MAEs of $f_1(x)$, $f_2(x)$, and $f_3(x)$ at $(a, b) = (3, 3)$ with different choices of $\mathcal{L}$. Figure 5 obtains the Log_{10} MAEs, AEs, and approximate errors of $f_1(x)$, $f_2(x)$, and $f_3(x)$ at $(a, b) = (3, 3)$ with $\mathcal{L} = 22$.

The results in Table 9 and Figure 5 confirm the high accuracy and convergence of the scheme presented here when applied to solve a system of Volterra-type integro-differential equations.

Table 9. MAEs of $f_1(x)$, $f_2(x)$, and $f_3(x)$ for problem (8.7).

$\mathcal{L}$	$f_1(x)$	$f_2(x)$	$f_3(x)$
4	5.1937×10^{-3}	6.5436×10^{-3}	6.1314×10^{-3}
8	3.2437×10^{-6}	4.9448×10^{-6}	4.1493×10^{-6}
12	3.9716×10^{-9}	6.0504×10^{-9}	5.0764×10^{-9}
16	4.5750×10^{-12}	6.9659×10^{-12}	5.8434×10^{-12}
20	5.3290×10^{-15}	8.3266×10^{-15}	6.4581×10^{-15}

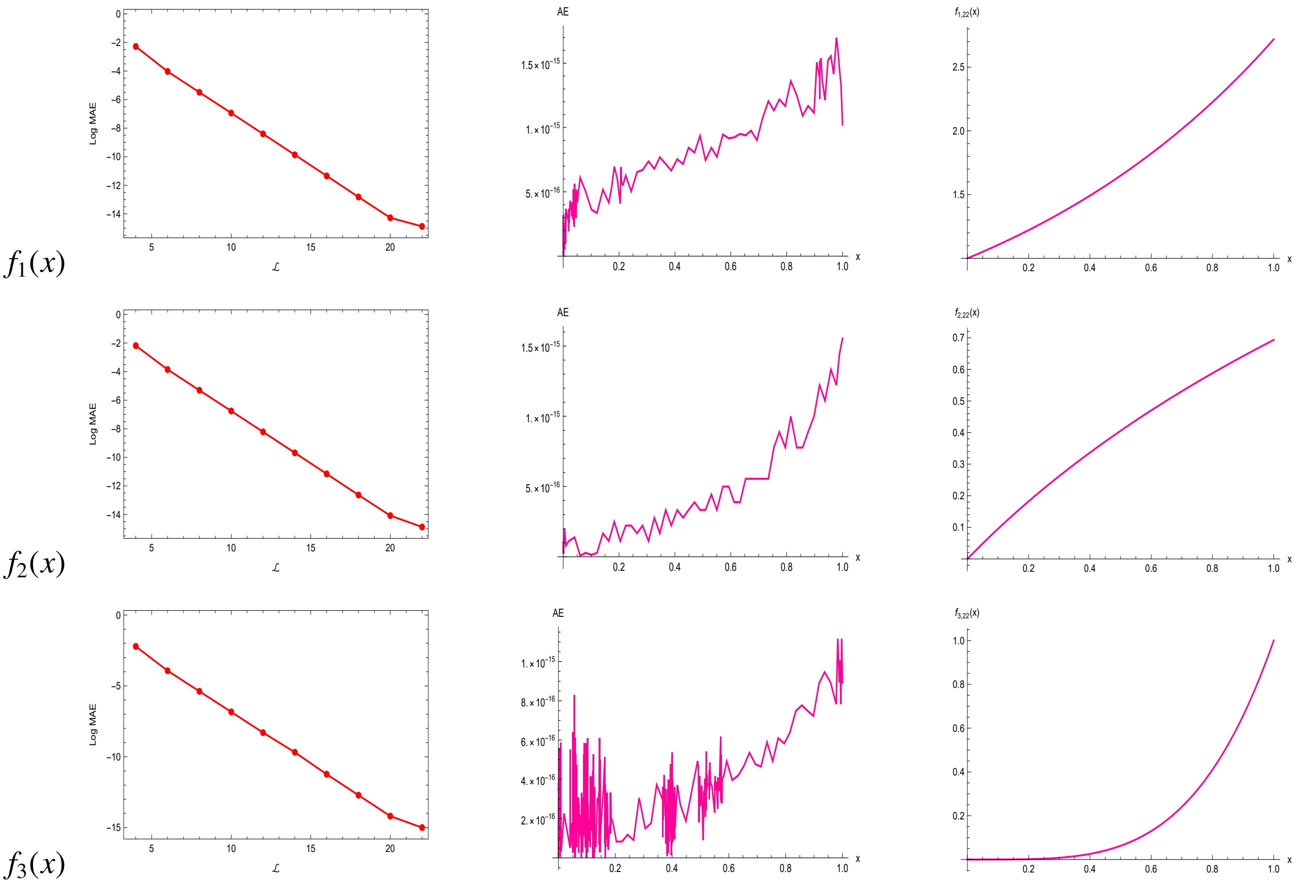

Figure 5. Log_{10} MAEs, AEs, and approximate solutions of $f_1(x)$, $f_2(x)$ and $f_3(x)$ for problem (8.7).

9. Conclusions

The current study introduces a numerical method for the multi-pantograph integro-differential equation. The operational matrices of integration, differentiation, and pantographs are implemented together with the shifted Jacobi Gauss quadrature rule and the spectral tau approach to convert the problem into a simpler one of solving a system of algebraic equations. According to the authors' research, this is the first work that discusses a numerical solution of the studied problems based on the tau spectral approach, and the operational matrices of integration, differentiation, and pantographs. Application of the spectral tau method together with the operational matrix technique guarantees a numerical solution of high accuracy and rapid convergence using a small number of Jacobi polynomial terms. The presented approach is extended to handle the two-dimensional case of the studied problem. The numerical results confirm the superiority of the presented numerical approaches compared with other spectral methods. Our future extension of the numerical scheme is the tempered fractional differential equations [30]. While the numerical results confirm exponential convergence for smooth solutions, a rigorous theoretical convergence analysis will be explored in subsequent work. This analysis will use established frameworks for Jacobi spectral methods, including those of [31, 32].

Author contributions

The authors declare that they have contributed equally to the conception, design, analysis, and writing of this manuscript. All authors read and approved the final manuscript.

Use of Generative-AI tools declaration

The authors declare they have not used Artificial Intelligence (AI) tools in the creation of this article.

Acknowledgments

This work was supported and funded by the Deanship of Scientific Research at Imam Mohammad Ibn Saud Islamic University (IMSIU) (grant number IMSIU-DDRSP2502).

Conflict of interest

The authors declare that they have no conflict of interest.

References

1. Y. Kuang, *Delay differential equations: With applications in population dynamics*, USA, New York: Academic Press, **91** (1993).
2. S. S. Ezz-Eldien, A. Alalyani, Legendre spectral collocation method for one-and two-dimensional nonlinear pantograph Volterra-Fredholm integro-differential equations, *Int. J. Mod. Phys. C*, **37** (2025), 2550061. https://doi.org/10.1142/s0129183125500615
3. M. Dehghan, F. Shakeri, The use of the decomposition procedure of adomian for solving a delay differential equation arising in electrodynamics, *Phys. Scripta*, **78** (2008), 065004. https://doi.org/10.1088/0031-8949/78/06/065004
4. L. Fox, D. F. Mayers, J. A. Ockendon, A. B. Tayler, On a functional differential equation, *IMA J. Appl. Math.*, **8** (1971), 271–307. https://doi.org/10.1093/imamat/8.3.271
5. J. R. Ockendon, A. B. Tayler, The dynamics of a current collection system for an electric locomotive, *Proc. R. Soc. A*, **322** (1971), 447–468. https://doi.org/10.1098/rspa.1971.0078
6. M. A. Zaky, I. G. Ameen, N. A. Elkot, E. H. Doha, A unified spectral collocation method for nonlinear systems of multi-dimensional integral equations with convergence analysis, *Appl. Numer. Math.*, **161** (2021), 27–45. https://doi.org/10.1016/j.apnum.2020.10.028
7. W. G. Ajello, H. I. Freedman, J. Wu, Analysis of a model representing stage-structured population growth with state-dependent time delay, *SIAM J. Appl. Math.*, **52** (1992), 855–869. https://doi.org/10.1137/0152048
8. M. A. Elkot, E. H. Doha, I. G. Ameen, G. Ibrahem, A. S. Hendy, M. A. Zaky, A re-scaling spectral collocation method for the nonlinear fractional pantograph delay differential equations with non-smooth solutions, *Commun. Nonlinear Sci.*, **118** (2023), 107017. https://doi.org/10.1016/j.cnsns.2022.107017

9. M. M. Alsuyuti, E. H. Doha, S. S. Ezz-Eldien, I. K. Youssef, Spectral Galerkin schemes for a class of multi-order fractional pantograph equations, *J. Comput. Appl. Math.*, **384** (2021), 113157. https://doi.org/10.1016/j.cam.2020.113157
10. G. A. Bocharov, F. A. Rihan, Numerical modelling in biosciences using delay differential equations, *J. Comput. Appl. Math.*, **125** (2000), 183–199. https://doi.org/10.1016/S0377-0427(00)00468-4
11. J. Zhao, Y. Cao, Y. Xu, Sinc numerical solution for pantograph Volterra delay-integro-differential equation, *Int. J. Comput. Math.*, **94** (2017), 853–865. https://doi.org/10.1080/00207160.2017.1283030
12. M. M. Alsuyuti, E. H. Doha, B. I. Bayoumi, S. S. Ezz-Eldien, Robust spectral treatment for time-fractional delay partial differential equations, *Comput. Appl. Math.*, **42** (2023), 159. https://doi.org/10.1007/s40314-023-02287-w
13. M. A. Zaky, Finite difference/fractional Pertrov-Galerkin spectral method for the linear time-space fractional reaction-diffusion equation, *Mathematics*, **13** (2025), 1864. https://doi.org/10.3390/math13111864
14. J. Zhao, Y. Cao, Y. Xu, Tau approximate solution of linear pantograph Volterra delay-integro-differential equation, *Comput. Appl. Math.*, **39** (2020), 46. https://doi.org/10.1007/s40314-020-1080-5
15. M. A. Zaky, I. G. Ameen, A novel Jacobi spectral method for multi-dimensional weakly singular nonlinear Volterra integral equations with nonsmooth solutions, *Eng. Comput.-Germany*, **37** (2021), 2623–2631. https://doi.org/10.1007/s00366-020-00953-9
16. J. G. Liu, W. H. Zhu, Y. K. Wu, G. H. Jin, Application of multivariate bilinear neural network method to fractional partial differential equations, *Res. Phys.*, **47** (2023), 106341. https://doi.org/10.1016/j.rinp.2023.106341
17. R. F. Zhang, S. Bilige, Bilinear neural network method to obtain the exact analytical solutions of nonlinear partial differential equations and its application to p-gBKP equation, *Nonlinear Dynam.*, **95** (2019), 3041–3048. https://doi.org/10.1007/s11071-018-04739-z
18. R. M. Zhong, Bilinear neural network method for obtaining the exact analytical solutions to nonlinear evolution equations and its application to KdV equation, *Afr. Diaspora J. Math.*, **27** (2024), 4. https://doi.org/10.7813/s3x0tb07
19. Y. Alkhezi, Y. H. R. Almubarak, A. Shafee, Neural-network-based approximations for investigating a Pantograph delay differential equation with application in Algebra, *Int. J. Math. Comput. Sci.*, **20** (2025), 195–209. https://doi.org/10.69793/ijmcs/01.2025/ahmad
20. X. R. Xie, R. F. Zhang, Neural network-based symbolic calculation approach for solving the Korteweg–de Vries equation, *Chaos Soliton. Fract.*, **194** (2025), 116232. https://doi.org/10.1016/j.chaos.2025.116232
21. T. Ji, J. Hou, C. Yang, The operational matrix of Chebyshev polynomials for solving pantograph-type Volterra integro-differential equations, *Adv. Contin. Discrete M.*, **2022** (2022), 57. https://doi.org/10.1186/s13662-022-03729-1
22. H. Jafari, N. Tuan, R. M. Ganji, A new numerical scheme for solving pantograph type nonlinear fractional integro-differential equations, *J. King Saud Univ. Sci.*, **33** (2021), 101185. https://doi.org/10.1016/j.jksus.2020.08.029

23. Y. Wang, S. S. Ezz-Eldien, A. A. Aldraiweesh, A new algorithm for the solution of nonlinear two-dimensional Volterra integro-differential equations of high-order, *J. Comput. Appl. Math.*, **364** (2020), 112301. https://doi.org/10.1016/j.cam.2019.06.017
24. P. Darania, F. M. Sotoudehmaram, Numerical analysis of a high order method for nonlinear delay integral equations, *J. Comput. Appl. Math.*, **374** (2020), 112738. https://doi.org/10.1016/j.cam.2020.112738
25. N. A. Elkot, M. A. Zaky, E. H. Doha, I. G. Ameen, On the rate of convergence of the Legendre spectral collocation method for multi-dimensional nonlinear Volterra–Fredholm integral equations, *Commun. Theor. Phys.*, **73** (2021), 025002. https://doi.org/10.1088/1572-9494/abcfb3
26. A. H. Tedjani, S. E. Alhazmi, S. S. Ezz-Eldien, An operational approach for one-and two-dimension high-order multi-pantograph Volterra integro-differential equation, *AIMS Math.*, **10** (2025), 9274–9294. https://doi.org/10.3934/math.2025426
27. M. A. Zaky, M. Babatin, M. Hammad, A. Akgül, A. S. Hendy, Efficient spectral collocation method for nonlinear systems of fractional pantograph delay differential equations, *AIMS Math.*, **9** (2017), 15246–15262. https://doi.10.3934/math.2024740
28. S. S. Ezz-Eldien, On solving fractional logistic populationmodels with applications, *Comput. Appl. Math.*, **37** (2018), 6392-–6409. https://doi.org/10.1007/s40314-018-0693-4
29. E. H. Doha, A. H. Bhrawy, D. Baleanu, S. S. Ezz-Eldien, The operational matrix formulation of the Jacobi tau approximation for space fractional diffusion equation, *Adv. Differ. Equ.*, **231** (2014). https://doi.org/10.1186/1687-1847-2014-231
30. M. A. Zaky, A. A. Kenany, S. E. Alhazmi, S. S. Ezz-Eldien, Numerical treatment of tempered space-fractional Zeldovich–Frank–Kamenetskii equation, *Rom. Rep. Phys.*, 2025.
31. J. Zhou, Z. Jiang, H. Xie, H. Niu, The error estimates of spectral methods for 1-dimension singularly perturbed problem, *Appl. Math. Lett.*, **100** (2020), 106001. https://doi.org/10.1016/j.aml.2019.106001
32. C. T. Sheng, Z. Q. Wang, B. Y. Guo, A multistep Legendre–Gauss spectral collocation method for nonlinear Volterra integral equations, *SIAM J. Numer. Anal.*, **52** (2014). https://doi.org/10.1137/130915200